HHS Public Access

Author manuscript

Cell Metab. Author manuscript; available in PMC 2023 August 02.

Published in final edited form as:

Cell Metab. 2022 August 02; 34(8): 1121–1136.e6. doi:10.1016/j.cmet.2022.07.002.

T-bet+ B cells accumulate in adipose tissue and exacerbate metabolic disorder during obesity

Thomas Hägglöf[1,#], **Carlo Vanz**[1,#], **Abigail Kumagai**[1], **Elizabeth Dudley**[1], **Vanessa Ortega**[1], **McKenzie Siller**[1], **Raksha Parthasarathy**[1], **Josh Keegan**[1], **Abigail Koenigs**[1], **Travis Shute**[1], **Elizabeth A. Leadbetter**[*,1]

[1]Department of Microbiology, Immunology & Molecular Genetics; UT Health; San Antonio, Texas, USA 78229

SUMMARY:

Obesity is accompanied by inflammation in adipose tissue, impaired glucose tolerance, and changes in adipose leukocyte populations. These studies of adipose tissue from humans and mice revealed that increased frequencies of T-bet$^+$ B cells in adipose tissue depend on invariant NKT cells and correlate with weight gain during obesity. Transfer of B cells enriched for T-bet$^+$ cells exacerbates metabolic disorder in obesity, while ablation of *Tbx21* specifically in B cells reduces serum IgG2c levels, inflammatory cytokines, and inflammatory macrophages in adipose tissue, ameliorating metabolic symptoms. Furthermore, transfer of serum or purified IgG from HFD mice restores metabolic disease in Tbet+ B cell deficient mice, confirming Tbet+ B cell-derived IgG as a key mediator of inflammation during obesity. Together, these findings reveal an important pathological role for T-bet$^+$ B cells, which should inform future immunotherapy design in type 2 diabetes and other inflammatory conditions.

eTOC blurb

Hägglöf et al. dissect the role of T-bet+ B cells in exacerbating metabolic disorder during obesity. Specifically, T-bet+ B cells accumulate during progressing obesity in mice and humans. B cell-targeted deletion of *Tbx21* significantly ameliorates metabolic disorder in obese mice, but it can be restored by transfer of HFD IgG.

Keywords

Obesity; Inflammation; Metabolic disorder; B cells; Type 2 diabetes; T-bet B cells; IgG2c

[*]Lead Contact: leadbetter@uthscsa.edu.

AUTHOR CONTRIBUTIONS

T.H., C.V., and E.A.L conceived and designed experiments, analyzed and interpreted data, wrote and edited the manuscript. T.H., C.V., A.K., J.K., T.S., V.O., M.S., R.P., and A.K. performed experiments. E.A.L directed the study and secured funding.

[#]Contributed equally

COMPETING INTERESTS STATEMENT

The authors declare no competing financial interests.

INTRODUCTION

Obesity causes chronic inflammation in adipose tissue, leading to impaired glucose tolerance and type 2 diabetes (T2D) (Osborn and Olefsky, 2012; Xu et al., 2003). Homeostasis is maintained in part by adipose immune cells, which are critical for the regulation of metabolic disorder (Bapat et al., 2015; Lynch, 2014; Mathis, 2013), including macrophages and lymphocytes.

To address whether B lymphocytes are beneficial or detrimental to diet-induced obesity (Nishimura et al., 2013; Winer et al., 2011; Wu et al., 2014), we investigated whether chronic inflammation during obesity preferentially activates a particular B cell subset. Chronic inflammation caused by infectious or autoimmune disease expands B cells that express CD11c and T-bet (Isnardi et al., 2010; Moir et al., 2008; Weiss et al., 2009). Splenic B cells that express T-bet also accumulate early in autoimmune settings (Manni et al., 2018), are expanded by the cytokines IFNγ and IL-21 (Naradikian et al., 2016; Rubtsov et al., 2011) as well as engagement of TLR7, TLR9, and the B cell receptor (Hao et al., 2011; Rubtsova et al., 2013). Tbet+ B cells identified during aging and obesity are defined by their lack of CD21 and CD23 (double negative B cells) and have been described as Age Associated B cells (ABCs) (Cancro, 2020; Frasca et al., 2021).

Another lymphocyte population, invariant Natural Killer T (iNKT) cells, are enriched in lean adipose tissue but gradually deplete during obesity (Lynch et al., 2009). INKT cells both negatively and positively regulate B cells depending on the immunological context (Enoksson et al., 2011; Hagglof et al., 2016; King et al., 2011; Leadbetter et al., 2008; Vomhof-DeKrey et al., 2015). INKT cells express invariant T cell receptors and respond rapidly to pathogen-stimulated danger signals, glycolipids in the context of antigen-presenting CD1 molecules, or both combined (Kohlgruber et al., 2016). INKT cells are critical regulatory cells capable of producing both proinflammatory and anti-inflammatory cytokines, and express IL-10 in part to maintain metabolic homeostasis. Many changes to $CD11c^+$ inflammatory myeloid cells, T regulatory- and iNKT cells in adipose tissue during obesity and T2D have been well characterized (Chawla et al., 2011; Lynch, 2014; Mathis, 2013; Osborn and Olefsky, 2012; Weisberg et al., 2003), but their interactions with adipose B cells remain undefined.

Herein we describe a role for T-bet^+ B cells in exacerbating metabolic disorder and diabetic symptoms during obesity. Adipose tissue T-bet^+ B cells accumulate in humans with increasing body mass index and in mice with increasing weight. T-bet^+ B cells constitute a B cell population with a distinct phenotype which can be expanded by iNKT cell activation during obesity, following TLR7 stimulation, or after glycolipid activation. Conditional knockout of T-bet in B cells improved glucose tolerance in mice on a high fat diet (HFD) diet, as compared to littermate controls. Reciprocally, transfer of B cells enriched for T-bet^+ $CD11c^+$ cells exacerbates metabolic indices and promotes inflammation. The T-bet-B cell program drives secretion of CXCL10, a known mediator of pancreatic β cell destruction. Mice lacking Tbet in their B cells gain less weight and accumulate fewer macrophages (especially M1 macrophages) in their adipose tissue, which can be reversed by adoptive transfer of HFD serum or purified IgG. In short, T-bet^+ B cells exacerbate the development

of metabolic disease through a combination of effects including secretion of pathogenic IgG. These findings provide insight into the pathophysiology of metabolic disorder in mice and humans during obesity and will inform rational design of future immunotherapies for obesity, T2D, and other inflammatory disorders.

RESULTS

B cells are activated in adipose tissue from patients that are overweight and obese

The makeup of human adipose tissue B cell subsets has been incompletely described. To characterize adipose tissue B cells, we isolated human leukocytes from subcutaneous adipose tissue resected from plastic surgery patients (Table S1). Using flow cytometry, we compared leukocytes extracted from adipose tissue from patients that are lean (body mass index [BMI] < 25 kg/m^2), overweight (BMI 25 – 30 kg/m^2), or obese (BMI > 30 kg/m^2) (Figure 1A). We detected no differences in the proportion of B cells but found a significant decrease in the proportion of iNKT cells in patients that are obese compared to patients that are lean or overweight, consistent with previous reports (Figure 1A, (Lynch et al., 2012)). We further identified a significant increase in B cell size (Forward scatter area; FSC-A) which correlated with increasing BMI (Figure 1B). The increase in cell size and correlation with BMI was not unique to B cells, as T cells displayed a similar correlation between cell size and BMI (Figure S1A).

The transcription factor T-bet is a master regulator of T_H1 lineage commitment (Szabo et al., 2000), but also regulates a subset of B cells which expands in chronic inflammation (Isnardi et al., 2010; Kenderes et al., 2018; Rubtsova et al., 2017). Given the state of chronic inflammation in adipose tissue from patients that are overweight and obese as compared to control patients that are lean (Xu et al., 2003), we investigated expression of T-bet in adipose tissue B cells. Flow cytometry revealed more intracellular T-bet protein in B cells from patients that are overweight or obese as compared to control patients that are lean (Figure 1C). The protein level of T-bet in B cells correlated with BMI (Figure 1C). We next measured cell surface α integrin glycoprotein CD11c on lymphocytes by flow cytometry and found significantly increased CD11c on B cells from patients that are overweight, but not patients that are obese, when compared to controls that are lean (Figure 1D). There was no correlation between CD11c expression by B cells and BMI (Figure 1D). When measuring expression of the early activation marker CD69 using flow cytometry, we found a similar pattern as for CD11c, where B cells from patients that are overweight expressed significantly higher amounts of CD69 as compared to patients that are lean or obese (Figure 1E). The changes in protein expression of T-bet, CD11c, and CD69 were specific to B cells, as there was a trend but no significant increases in Tbet protein expression for $CD3^+$ T cells from matched donors (Figure S1B-D). T-bet-expressing B cells have previously been studied in the context of autoimmunity and aging (Hao et al., 2011; Rubtsov et al., 2011). Therefore, we investigated potential correlations between age and adipose B cell expression of activation markers. Surprisingly, flow cytometry showed no correlation between age and activation marker expression by adipose B cells or T cells (Figure S1E-H). Instead, the main determinant of an activated phenotype by adipose tissue lymphocytes was BMI. Thus, BMI

correlates with B cell activation and increased T-bet expression by human adipose tissue B cells.

Obesity-induced T-bet$^+$ B cell accumulation is conserved in mouse and human adipose tissue

We next investigated whether the correlation between BMI and T-bet expression in total human adipose tissue B cells could be accounted for by the expansion of a subset of T-bet$^+$ of B cells. Flow cytometry revealed an increase in Tbet expression by B cells (Figure 1F), as well as a significantly higher proportion of T-bet$^+$ B cells in subcutaneous adipose tissue from overweight and obese patients as compared to lean patients (Figure 1G). There was no correlation between the proportion of T-bet$^+$ B cells in adipose tissue and patient age (Figure 1H). However, there was a significant correlation between BMI and frequency of T-bet$^+$ B cells in human adipose tissue (Figure 1I), identifying BMI, but not age, as the key factor influencing the accumulation of T-bet$^+$ B cells in human adipose tissue during obesity.

Next, we used flow cytometry to phenotype T-bet$^+$ B cells and T-bet$^-$ B cells from the same patients. We found that T-bet$^+$ B cells from patients that are overweight and obese expressed significantly higher surface levels of CD11c as compared to T-bet$^-$ B cells from the same patient, and there was a similar trend in lean patients (Figure 1J). Thus, Tbet+ B cells are CD11c+ even in lean mice. T-bet$^+$ B cells from patients that are overweight and obese showed increased cell size (FSC-A) as well as increased expression of the leukocyte activation markers CD69 and Nur77 as compared to T-bet$^-$ B cells from within the same patients. There were no comparable changes in protein expression in patients that are lean (Figure S2). We next noted there were no differences in the surface expression of glycolipid antigen presenting molecule CD1c comparing T-bet$^+$ and T-bet$^-$ B lymphocytes in any patient subgroup (Figure S2). However, in patients that are obese, T-bet$^+$ B cells expressed significantly less CD1d protein than T-bet$^-$ B cells from the same donors (Figure 1K). Patients that are overweight exhibited a similar trend in CD1d downregulation by T-bet$^+$ B cells compared to T-bet$^-$ B cells from the same donor. T-bet$^+$ B cells have been reported to express lower levels of CD27 than memory B cells (Wang et al., 2018). T-bet$^+$ B cells in our study expressed modestly lower surface amounts of CD27 as compared to T-bet$^-$ B cells from the same patient, although not statistically significant (Figure S2). Thus, T-bet$^+$ B cells from patients that are overweight and obese display features of activated B cells, including upregulation of CD11c, CD69, and Nur77.

Since T-bet$^+$ B cells accumulate in adipose tissue from patients that are overweight and obese, we next utilized an *in vivo* mouse model to dissect the function of T-bet$^+$ B cells and mechanisms governing their accumulation. To this end, C57BL/6 wild-type mice were fed a high fat diet (HFD) for at least 8 weeks to induce obesity, metabolic disorder, and accompanying symptoms of T2D (Winzell and Ahren, 2004). Mice on a HFD consistently gained significantly more body weight than control mice on a normal chow diet (NCD) (Figure 2A). As expected, epididymal white adipose tissue (WAT) weight increased significantly in mice fed a HFD as compared to NCD controls (Figure 2A). HFD-fed mice also displayed increased concentrations of resting serum glucose and impaired glucose tolerance as measured by the glucose tolerance test (GTT), compared to NCD-fed mice

(Figure 2B). Flow cytometry revealed that obese HFD-fed mice mirrored humans that are overweight and obese in that they had no differences in the frequencies of total B cells in WAT or spleen compared to lean controls (Figure 2C). There were also no differences in numbers of total B cells in NCD vs HFD WAT, but very modest increases in total B cells in spleens from HFD fed mice compared to NCD mice (Figure 2C). However, just like patients that are overweight and obese, obese HFD fed mice have a significantly higher frequency and number of T-bet$^+$ CD11c$^+$ B cells in adipose tissue than lean mice fed a NCD (Figure 2D). T-bet$^+$ CD11c$^+$ B cells also accumulated in the spleens of obese HFD fed mice as compared to lean NCD mice (Figure 2E). Similar to humans, frequencies of T-bet$^+$ CD11c$^+$ B cells in adipose tissue and spleen correlated significantly with total body mass (Figure 2D–E).

We next used flow cytometry to compare phenotypes of T-bet$^+$ CD11c$^+$ B cells to T-bet$^-$ CD11c$^-$ B cells from the same mouse. HFD-expanded mouse T-bet$^+$ CD11c$^+$ B cells displayed a similar phenotypic profile as T-bet$^+$ B cells from patients that are obese or overweight. T-bet$^+$ CD11c$^+$ B cells were larger and expressed higher protein amounts of CD69 and intracellular Nur77, compared to T-bet$^-$ CD11c$^-$ B cells (Figure 2F–H). T-bet$^+$ CD11c$^+$ B cells also expressed lower protein amounts of the complement receptor CD21, and the low-affinity IgE receptor CD23, compared to T-bet$^-$ CD11c$^-$ B cells from the same mouse (Figure 2I–J). Flow cytometry revealed no significant differences in other splenic B cell subset frequencies in obese HFD-fed mice as compared to lean NCD-fed mice (Figure S3A-B). Similar to humans with obesity, T-bet$^+$ CD11c$^+$ B cells from obese HFD-fed mice expressed significantly lower levels of CD1d as compared to T-bet$^-$ CD11c$^-$ B cells from the same mouse, while there were no significant differences in CD1d expression between these two B cell populations in lean NCD-fed mice (Figure 2K). Thus, activated T-bet$^+$ CD11c$^+$ B cells are implicated in the modulation of metabolic disorders across species.

INKT cells support expansion of T-bet$^+$ CD11c$^+$ B cells during obesity

We found lower amounts of CD1d on the surface of T-bet$^+$ B cells compared to T-bet$^-$ B cells in both mouse and human adipose tissue in obesity. We next investigated whether CD1d-restricted iNKT cells affected the accumulation T-bet$^+$ CD11c$^+$ B cells in HFD-fed mice by performing an unsupervised dimensionality reduction analysis of flow cytometry data using the t-distributed stochastic neighboring embedding (tSNE) algorithm (van der Maaten and Hinton, 2008). Data were acquired using wild-type and iNKT cell-deficient *Cd1d1*$^{-/-}$ splenocytes from lean NCD or obese HFD mice labeled with lineage markers for B cells, T cells, and iNKT cells as well as Tbet and CD11c. The tSNE algorithm identified a distinct subset of CD19$^+$ B220$^+$ B cells (Figure 3A, “B cell cluster 2”, see also Figure S4) which segregated from the major cluster of CD19$^+$ B220$^+$ cells (Figure 3A, “B cell cluster 1”). B cell cluster 2 expressed higher protein amounts of T-bet and CD11c than B cell cluster 1 (Figure 3A). Interestingly, we found that our previously observed increase in T-bet$^+$ CD11c$^+$ B cell frequency in adipose tissue from wild-type HFD-fed obese mice compared to lean NCD-fed mice was missing in *Cd1d1*$^{-/-}$ HFD-fed mice (Figure 3B). Furthermore, there was a similar lack of expansion of T-bet$^+$ CD11c$^+$ B cell frequency in spleen from obese *Cd1d1*$^{-/-}$ HFD-fed mice, compared to obese wild-type HFD-fed mice (Figure 3C). Thus, even though adipose iNKT cell numbers dwindle with increasing obesity, their limited

presence is required to expand T-bet$^+$ B cells in obesity. Because of this dichotomy, we next examined the nature of the iNKT cells remaining in adipose tissue of WT HFD mice. Interestingly, the obese adipose iNKT cells were skewed towards the more inflammatory IFNγ-producing NK1.1^{pos} iNKT subset (Figure 3H), rather than the more regulatory IL-10 producing NK1.1^{neg} iNKT subset (LaMarche et al., 2020).

T-bet$^+$ CD11c$^+$ B cells play a role in the context of viral infection and autoimmune disorders, where they produce immunoglobulin (Ig) G2c during disease progression or infection (Barnett et al., 2016; Peng et al., 2002; Rubtsova et al., 2017; Rubtsova et al., 2013). Therefore, we measured serum Ig titers by ELISA from wild-type and iNKT cell-deficient *Cd1d1*$^{-/-}$ mice fed the NCD or the HFD. We found that obese HFD-fed wild-type mice had higher titers of IgG2c and IgM than lean NCD-fed wild-type controls, while there were no differences in IgG1 (Figure 3D–F). A similar increase was not detectable in IgG2c or IgM in *Cd1d1*$^{-/-}$ obese HFD-fed mice, when compared to controls (Figure 3D–F). There was also a significant correlation between the proportion of T-bet$^+$ CD11c$^+$ B cells in the spleen and serum concentrations of IgM and IgG2c when wild-type and *Cd1d1*$^{-/-}$ serum samples were pooled for statistical analysis (Figure 3D–F). Our findings indicate that T-bet$^+$ CD11c$^+$ B cell expansion as well as IgG2c and IgM production in obesity is supported by iNKT cells, an inflammatory subset capable of producing IFNγ.

Innate signaling drives T-bet$^+$ CD11c$^+$ B cell expansion and is iNKT cell-dependent

We next considered whether other means of inducing T-bet$^+$ CD11c$^+$ B cell expansion also require iNKT cells. Stimulation through TLR7 potently upregulates T-bet in B cells *in vitro* (Naradikian et al., 2016; Rubtsova et al., 2013). To assess the effect of TLR7 activation on B cells *in vivo*, we injected wild-type mice intraperitoneally (i.p.) with 50 μg of the TLR7 agonist R848 on day 0 and day 2 and harvested spleens on day 4. Flow cytometry revealed that B cells from mice injected with R848 increased in size (FSC-A), upregulated T-bet, CD69, and CD86 protein levels, while CD21, CD23, and CD1d protein levels were downregulated, as compared to naïve control mice (Figure 4A). To confirm the specific ability of TLR7 engagement to drive T-bet$^+$ B cell expansion, we next injected mice with R848 and used flow cytometry to reveal a significant increase in the proportion of B cells that were expressing CD11c or both Tbet and CD11c as well as CD138$^+$ plasmablasts, when compared to naïve control mice (Figure 4B–G). Concomitant with the increase in CD11c+/ T-bet$^+$ CD11c$^+$ B cells was a significant decrease in transitional type 2 (T2) and transitional type 2 – marginal zone precursor (T2-MZP) B cells, suggesting a possible developmental transition from T2 or T2-MZP into the T-bet$^+$ CD11c$^+$ B cell population. There were no generalized differences in the proportions of transitional type 1 (T1), marginal zone B (MZB), follicular B (FOB), germinal center B (GC B) cells, or CD21$^-$ CD23$^-$ B cells between R848-treated and untreated mice (Figure 4H). These results demonstrate TLR7 engagement can drive expansion of T-bet$^+$ CD11c$^+$ B cells, possibly seeded from precursor subsets in the spleen.

To investigate if TLR7-driven expansion of T-bet-expressing B cells was also supported by iNKT cells, used flow cytometry to reveal a significant expansion of T-bet$^+$ CD11c$^+$ B cell frequency in wild-type mice injected with R848, while iNKT cell-deficient *Cd1d1*$^{-/-}$ mice

showed a modest but not statistically significant accumulation of T-bet$^+$ CD11c$^+$ B cells in response to R848 (Figure 4I). Because T-bet$^+$ CD11c$^+$ B cell expansion can depend in part on IFNγ, and TLR7 signaling induces iNKT cells to produce IFNγ (Van et al., 2011), we assessed whether iNKT cells were a potential source of IFNγ in this system. Specifically, we used flow cytometry to assess eYFP+ expression in IFNγ–reporter mice (Reinhardt et al., 2009) and found a significant increase in IFNγ-expressing iNKT cells in injected with R848 as compared to naïve animals, while conventional T cells displayed no parallel increase in IFNγ (Figure 4J).

Because glycolipid activation of iNKT cells induces IFNγ production, we next tested whether direct activation of iNKT cells could expand T-bet$^+$ CD11c$^+$ B cells. To this end, we injected wild-type and iNKT cell-deficient *Jα18*$^{-/-}$ mice i.p. with 0.5 μg of the iNKT cell-specific ligand alpha-galactosylceramide (α–GalCer) and measured expansion of splenic T-bet$^+$ CD11c$^+$ B cells 4 days later. As expected, flow cytometry revealed a significant accumulation of T-bet$^+$ CD11c$^+$ B cells in wild-type mice injected with α–GalCer compared to naïve controls. However, we did not detect a significant accumulation of T-bet$^+$ CD11c$^+$ B cells in iNKT cell-deficient *Jα18*$^{-/-}$ mice (Figure 4K). Thus, iNKT cell-specific activation by glycolipids, well documented to stimulate IFNγ secretion by iNKT cells, supports expansion of T-bet$^+$ CD11c$^+$ B cells.

T-bet$^+$ B cells secrete CXCL10 and exacerbate metabolic disorder in obesity

Previous transcriptomic data identified increased amounts of *Cxcl10* mRNA in T-bet-expressing CD11b$^+$ B cells as compared to follicular B cells (Rubtsov et al., 2011) and found that IFNγ induced *Cxcl10* transcripts in cultured follicular B cells (Naradikian et al., 2016). To test if T-bet-expressing B cells secrete CXCL10 protein, we stimulated isolated B cells *in vitro* with 2.5 μg/ml R848 or medium alone for 2 days. Flow cytometry revealed that isolated B cells cultured with R848 *in vitro* adopted a phenotype similar to B cells stimulated with R848 *in vivo*: increased cell size (FSC-A), T-bet, CD69, and CD86 protein expression, as well as lower CD21 and CD1d protein expression, compared to medium alone (Figure 5A). ELISA revealed that *in vitro* culture with R848 increased B cell secretion of the chemokine CXCL10, when compared to medium alone (Figure 5B). To determine if CXCL10 is also produced *in vivo* in response to R848, we injected wild-type mice with R848 and measured serum concentration of CXCL10 by ELISA. Consistent with our *in vitro* results, we saw a significant increase in serum CXCL10 in mice injected with R848 as compared to naïve controls (Figure 5C).

CXCL10 and other B cell factors have been previously described to exacerbate T2D and metabolic disease (Schulthess et al., 2009), so we next assessed whether activated B cells enriched for T-bet$^+$ CD11c$^+$ cells played a role in the development of metabolic disorder during obesity. Concomitant TLR7, BCR, and IFNγ-receptor stimulation is an effective way to upregulate T-bet in B cells (Rubtsova et al., 2013). Therefore, we injected B1–8^{hi} mice transgenic for expression of a BCR specific for the hapten 4-hydroxy-3-nitrophenylacetyl (NP) (Shih et al., 2002) with NP conjugated to the carrier protein Keyhole limpet hemocyanin (KLH) plus R848 on day 0, and boosted with R848 on day 3 (Figure S5A). As expected, this regimen generated a pronounced accumulation of T-bet$^+$ CD11c$^+$ B cells

in the spleen on day 4, compared to naïve mice (Figure S5B), when B cells were isolated for transfer to lean or obese recipients. Following adoptive transfer of 10^7 B cells, mice were continued on their indicated diet for 4 more days, whereupon glucose tolerance was assessed (Figure S5C-D). GTT measurements detected no significant difference for lean NCD-fed mice that received B cells enriched for T-bet$^+$ CD11c$^+$ B cells using NP-KLH/R848 compared to mice receiving naïve B cells or no cell transfer (Figure 5D and Figure S5C). Strikingly, transfer of T-bet$^+$ CD11c$^+$ enriched B cells into obese mice fed a HFD significantly impaired glucose tolerance when compared to comparable mice receiving no cell transfer (Figure 5E and Figure S5D). Interestingly, transfer of B cells isolated from naïve mice into obese HFD-fed mice induced a similar exacerbation of glucose intolerance as compared to HFD-fed mice receiving R848-expanded B cells, suggesting the handling and transfer of B cells from naïve animals may activate existing low levels of Tbet+ B cells enough to exacerbate glucose intolerance even without R848 expansion (Figure S5D). Donor cells from both groups survived the transfer and were detected by congenic marker in recipient mice at frequencies consistent with the number of cells transferred (Figure S5E-F).

Ablation of *Tbx21* in B cells limits CXCL10 expression and metabolic disorder in obesity

Next, to directly investigate the role of T-bet-expressing B cells in the development of metabolic disorder during obesity, we abrogated T-bet (encoded by *Tbx21*) expression specifically in B cells by crossing *Tbx21*$^{flox/flox}$ mice (Intlekofer et al., 2008) with animals expressing Cre recombinase under the control of the promoter of *Cd19* (Rickert et al., 1997). To confirm that these mice lacked T-bet expression specifically in B cells, we harvested splenocytes from homozygous Tbet-deficient mice (*Tbx21*$^{flox/flox}$ *Cd19*$^{Cre/Cre}$), Tbet-heterozygous mice (*Tbx21*$^{flox/flox}$ *Cd19*$^{Cre/+}$) or T-bet intact (*Tbx21*$^{wt/wt}$ *Cd19*$^{Cre/+}$) littermate control mice and confirmed absence of intracellular expression of T-bet protein in B cells, but not T cells, of genetically deficient mice using flow cytometry (Figure S5G). We further confirmed an absence of Tbet specifically in the B cell subset by detecting *Tbx21* genomic DNA using gPCR on DNA isolated from tail tissue, negatively-selected B cells, or non-B cells from spleen in homozygous Tbet-deficient mice (*Tbx21*$^{flox/flox}$ *Cd19*$^{Cre/Cre}$), Tbet-heterozygous mice (*Tbx21*$^{flox/flox}$ *Cd19*$^{Cre/+}$) or T-bet intact (*Tbx21*$^{wt/wt}$ *Cd19*$^{Cre/+}$) littermate control mice (Figure S5H). Furthermore, we also used flow cytometry to examine T-bet expression following activation of splenic B cells. In intact *Tbx21*$^{wt/wt}$ *Cd19*$^{Cre/+}$ littermate control mice injected with R848, B cells upregulated T-bet as compared to naive controls (Figure S5I), similar to what we found previously (Figure 4A). On the contrary, R848 immunization did not induce T-bet expression in T-bet deficient B cells from *Tbx21*$^{flox/flox}$ *Cd19*$^{Cre/+}$ mice (Figure S5E). We used flow cytometry to confirm that the targeted deletion of *Tbx21* was specific for B cells, documenting T-bet upregulation in iNKT cells from both *Tbx21*$^{flox/flox}$ *Cd19*$^{Cre/+}$ mice and *Tbx21*$^{wt/wt}$ *Cd19*$^{Cre/+}$ littermate control mice activated with R848(Figure S5F). Thus, *Tbx21*$^{flox/flox}$ *Cd19*$^{Cre/+}$ mice fail to express T-bet specifically in B cells, while *Tbx21*$^{+/+}$ *Cd19*$^{Cre/+}$ littermate control mice express T-bet normally.

In vitro stimulation of B cells via TLR7 induces T-bet and secretion of CXCL10, so we next measured expression of CXCL10 in B cells lacking T-bet. At steady state in lean mice, T-bet$^+$ CD11c$^+$ B cells expressed significantly higher amounts of CXCL10 protein

than conventional B cells from the same mouse (Figure 6A). Since the majority of murine CD11c$^+$ B cells express T-bet (Figure 2E), we used CD11c expression as a surrogate for T-bet to evaluate CXCL10 expression in this subset of B cells following the targeted deletion of T-bet. Using flow cytometry we found that intact *Tbx21*$^{wt/wt}$ *Cd19*$^{Cre/+}$ mice on the HFD displayed a significant increase in the frequency of CXCL10$^+$ CD11c$^+$ B cells in spleen compared to their littermates fed the NCD (Figure 6B). Importantly, deficient *Tbx21*$^{flox/flox}$ *Cd19*$^{Cre/+}$ mice fed the HFD completely failed to accumulate splenic CXCL10$^+$ CD11c$^+$ B cells compared to littermate control mice (Figure 6B).

Finally, we evaluated whether T-bet B cell deficiency affects clinical symptoms of metabolic disease. Strikingly, obese *Tbx21*$^{flox/flox}$ *Cd19*$^{Cre/+}$ mice lacking T-bet$^+$ CXCL10$^+$ B cells and fed a HFD showed significantly improved glucose tolerance when compared to obese HFD-fed *Tbx21*$^{wt/wt}$ *Cd19*$^{Cre/+}$ littermate control mice (Figure 6C). Notably, lacking T-bet$^+$ B cells even modestly reduced GTT in lean mice (Figure 6D).

The data in this study has been collected from exclusively female patients and predominantly female mice. Accumulation of T-bet$^+$ CD11c$^+$ B cells in the spleen during obesity was more pronounced in female mice than male mice and, correspondingly, improvement of glucose tolerance (GTT) in mice with *Tbx21* conditionally knocked out in B cells was only detected in female mice (Figure 5). In contrast, male mice had a more modest increase in splenic T-bet$^+$ CD11c$^+$ B cell frequency during obesity, and showed no improvement in glucose tolerance upon conditional knockout of *Tbx21* in B cells during obesity (Figure S5K).

To understand the mechanism utilized by Tbet+ B cells to exacerbate disease, we further characterized the immunometabolic landscape of the *Tbx21*$^{flox/flox}$ *Cd19*$^{Cre/+}$ mice. We first noted that *Tbx21*$^{flox/flox}$ *Cd19*$^{Cre/+}$ mice placed on a high fat diet gained less weight than their WT counterparts (Figure 6E). The reduced weight gain in *Tbx21*$^{flox/flox}$ *Cd19*$^{Cre/+}$ mice was evident in both total body weight and visceral WAT (Figure 6F). The weight differential between these mice was not a consequence of reduced lipid storage by Tbet+ B cell deficient mice. Instead, we found a modest increase in lipid storage in both liver and adipose tissue. Increased lipid staining was detected in *Tbx21*$^{flox/flox}$ *Cd19*$^{Cre/+}$ mice as compared to intact WT mice using Oil Red O staining of liver tissue from both lean and obese animals (Figure S6 A-B). Similarly, adipocyte diameter was modestly increased in *Tbx21*$^{flox/flox}$ *Cd19*$^{Cre/+}$ mice compared to WT mice when placed on a HFD (Figure S6C-D). To examine the role of Tbet+ B cell derived CXCL10 in these weight or lipid storage differences, we created mixed BM chimeras with CXCL10 sufficient, or CXCL10 deficient, Tbet+ B cells. To isolate the CXCL10 deficiency to Tbet+ B cells, we reconstituted lethally irradiated *Tbx21*$^{flox/flox}$ *Cd19*$^{Cre/+}$ mice with a combination of *Tbx21*$^{flox/flox}$ *Cd19*$^{Cre/+}$ BM plus CXCL10−/− or CXCL10+/+ BM (Figure S7A). Following 9 weeks of reconstitution and 8 weeks of HFD feeding, both groups of mice were found to have similar metabolic responses to a GTT (Figure S7B). Instead, mice lacking CXCL10 in their Tbet+ B cells had a lower food intake than CXCL10 intact controls in the early weeks of their HFD feeding and gained less weight over the course of the testing (Figure S7C-E) suggesting CXCL10 secretion by Tbet+ B cells stimulates early weight gain during obesity rather than later inflammatory changes.

Tbet+ B cells instigate additional changes in adipose leukocyte populations during obesity. Flow cytometry confirmed increases in total CD45+ leukocyte WAT populations following HFD feeding in intact mice, but not in mice lacking Tbet+ B cells (Figure 6G). Dissecting the WAT populations more specifically revealed increases in adipose tissue macrophages during HFD feeding for intact littermate control mice, but not deficient *Tbx21*$^{flox/flox}$ *Cd19*$^{Cre/+}$ mice (Figure 6H). During HFD in intact littermate controls, more than 50% of the adipose macrophages were M1 inflammatory macrophages, which was similar for the *Tbx21*$^{flox/flox}$ *Cd19*$^{Cre/+}$ mice, suggesting that while macrophage frequency was reduced, macrophages that did enter the adipose assumed the expected inflammatory phenotype (Figure 6I).

ELISA revealed that both lean and obese *Tbx21*$^{flox/flox}$ *Cd19*$^{Cre/+}$ mice developed normal levels of total IgM and IgG [Figure 7A,B]. Tbet+ B cells typically produce IgG2c immunoglobulin in mice, so as expected, both lean and obese Tbet+ B cell deficient mice developed normal levels of total serum IgG1, but had reduced levels of IgG2c [Figure 7C, D]. Given previous evidence that Tbet+ B cell derived IgG2c can be pathogenic during disease (Rubtsova et al., 2017), we next considered the potential of Tbet-derived IgG2c to contribute to metabolic disease. Transfer of serum from obese WT mice to *Tbx21*$^{flox/flox}$ *Cd19*$^{Cre/+}$ mice increased glucose tolerance and moderately elevated resting glucose levels [Figure 7E, F]. The effect of the HFD serum could be attributed to the immunoglobulin, because transfer of IgG isolated from HFD serum significantly increased glucose tolerance of *Tbx21*$^{flox/flox}$ *Cd19*$^{Cre/+}$ mice [Figure 7E, F]. WAT macrophages are reduced in *Tbx21*$^{flox/flox}$ *Cd19*$^{Cre/+}$ mice compared to littermate controls, but the frequency and number of F480+CD11b+ macrophages can be restored by adoptive transfer of serum IgG from HFD mice [Figure 7H]. In summary, T-bet+ B cells produce IgG2c which exacerbates metabolic disorder during obesity, in part by recruiting adipose tissue macrophages. Together, these data examine the pathologic role of a key subset of B cells in obesity and identify a novel target for future immunotherapeutics aimed at reversing the development of metabolic disorder in obesity and T2D.

DISCUSSION

T-bet is a transcription factor well-known to affect B cell functions (Szabo et al., 2000). T-bet^{+} B cells and their antibodies have been described in aging and autoimmune disorders (Hao et al., 2011; Isnardi et al., 2010; Rubtsov et al., 2011; Rubtsova et al., 2017; Wang et al., 2018), but detailed characterization of directly pathogenic roles of these cells remains elusive. Here we discovered that T-bet^{+} B cells drive inflammation and exacerbate metabolic disorder during obesity. T-bet^{+} B cells accumulate in adipose tissue from humans and mice with obesity, and the frequencies of T-bet^{+} B cells correlate with increasing BMI or body weight, respectively. However, there was no correlation between accumulation of T-bet^{+} B cells and age. These findings suggest that B cell-stimulatory cues provided by the inflammatory adipose milieu during obesity may dominate those presented by aging.

Adipose tissue B cells from subjects that are overweight upregulate CD11c and CD69 compared to lean controls, while B cells from subjects that are obese no longer upregulated these activation markers. We hypothesize that progressing obesity-associated inflammation

initially activates adipose tissue B cells but leads to subsequent cellular exhaustion due to chronic inflammation in patients with obesity, reminiscent of observations from patients that are chronically infected or suffer from autoimmunity (Ehrhardt et al., 2005; Isnardi et al., 2010; Moir et al., 2008).

T-bet$^+$ B cells isolated from subjects that are overweight or obese exhibit a distinct phenotype compared to T-bet$^-$ B cells from the same donors, with many traits shared between human and mouse. Strikingly, T-bet$^+$ B cells in humans with obesity or mice on the HFD express lower amounts of the glycolipid-presenting molecule CD1d compared to T-bet$^-$ B cells from matched subjects. TLR7 stimulation induced a B cell phenotype with increased expression of T-bet, CD69, and CD86, but downregulation of CD21 and CD1d. Interestingly, expansion of T-bet$^+$ CD11c$^+$ B cells via TLR7 ligation, injection of α–GalCer, or during obesity were all iNKT cell-dependent. Ostensibly, the mechanism through which iNKT cells support T-bet$^+$ CD11c$^+$ B cells works in a cytokine-mediated non-cognate fashion, as the B cell T-bet program is associated with a downregulation of CD1d. Interestingly, TLR7 deficient mice are protected from metabolic abnormalities including weight gain, insulin resistance, and liver inflammation (Hanna Kazazian et al., 2019), suggesting that engagement through TLR7 may expand an inflammatory cell population which contributes to metabolic disease, which is consistent with our identification of an expanded population of Tbet+ B cells as contributors to metabolic disease.

Earlier *in vitro* studies established that TLR, cytokine, and BCR signals synergize to induce T-bet expression by B cells (Cancro, 2020; Naradikian et al., 2016; Rubtsova et al., 2013). We find that T-bet$^+$ CD11c$^+$ B cells are further supported by iNKT cells during the diet-induced inflammation of obesity, likely due to iNKT cell production of IL-21 and IFNγ (Grela et al., 2011). However, complementary signals may also contribute to the induction of T-bet in B cells during obesity. For example, saturated fatty acids (FA) stimulate TLR signaling and polyunsaturated FA inhibit TLR signaling (Lee et al., 2004). Obese individuals have higher concentrations of circulating saturated FA than lean individuals (Guerendiain et al., 2018), potentially driving their increased B cell-expression of T-bet. Alternatively, B cells could engage obesity-associated inflammatory cell debris through cognate recognition via their BCR. We found T-bet$^+$ CD11c$^+$ B cells to express more Nur77 protein compared to conventional B cells. As Nur77 expression directly correlates with BCR signaling strength (Ashouri and Weiss, 2017), this suggests increased exposure to cognate B cell antigen in adipose tissue and subsequent BCR-mediated induction of T-bet. Thus, qualitative and quantitative changes in lipid composition or cell destruction associated with obesity could provide TLR and BCR signals to induce T-bet$^+$ B cells with the aid of IFNγ or other cytokines from iNKT cells.

Interestingly, we also found increased serum amounts of IgM and IgG2c in obese wild-type mice compared to lean controls, which correlated with the T-bet$^+$ CD11c$^+$ B cell frequency, consistent with observations linking IgG2c production to T-bet-expressing B cells (Peng et al., 2002). Immunoglobulins can contribute to both pathologic and protective aspects of metabolic disease (Harmon et al., 2016; Shen et al., 2015; Winer et al., 2011). Our data is consistent with a detrimental role for T-bet$^+$ CD11c$^+$ B cells, and their antibody products, in obesity. Our demonstration that T-bet$^+$ B cells accumulate during obesity corroborates

earlier findings by Winer et al and Frasca et al and provides an explanation for previously observed increases specifically in IgG2c in VAT lysates extracted from mice on a HFD (Winer et al., 2011).

T-bet-expressing B cells activated via TLR7 secrete the proinflammatory chemokine CXCL10, consistent with earlier transcriptomic data and human studies (Agrawal and Gupta, 2011; Naradikian et al., 2016; Rubtsov et al., 2011). Interestingly, transfer of enriched T-bet^{+} CD11c^{+} B cells to obese HFD-fed mice significantly exacerbated glucose intolerance. Conversely, B cell-specific ablation of *Tbx21* reduced weight gain and significantly ameliorated metabolic disorder in HFD-fed obese mice, as compared to wild-type littermate control mice on the HFD. Using CXCL10 as a surrogate for Tbet+ expression, flow cytometry confirmed that *Tbx21*$^{flox/flox}$ *Cd19*$^{Cre/+}$ mice fed a HFD showed a complete lack of accumulation of CXCL10^{+} CD11c^{+} B cells in spleen compared to HFD-fed *Tbx21*$^{wt/wt}$ *Cd19*$^{Cre/+}$ littermate control mice. Restricting CXCL10 deficiency to Tbet+ B cells revealed an important role for CXCL10 in early weight gain during high fat diet feeding. Multiple additional roles for CXCL10 have previously been demonstrated in metabolic disease. For example, injection of CXCL10 can exacerbate glucose intolerance through impairment of β cell function and viability (Schulthess et al., 2009) and CXCL10 can cause macrophages to switch from an alternatively activated M2 phenotype to a more inflammatory M1 phenotype (Tomita et al., 2016). Thus, Tbet+ B cell-derived CXCL10 may uniquely contribute to weight gain, but could affect pancreatic β cells and macrophages through a mechanism redundant with other sources of CXCL10.

We further characterized a specific role for Tbet+ B cell-derived IgG2c to exacerbate metabolic disease in vivo during obesity. While removal of Tbet+ B cells reduces metabolic disease in obese mice, glucose intolerance can be restored by transfer of HFD serum or purified IgG from serum of obese mice. This reductionist approach reveals pathologic immunoglobulin to be the primary mechanism of Tbet+ B cell inflammation during obesity. Previous studies have characterized autoreactive IgG in serum from obese or T2D humans (Winer et al, 2011), but this is the first specific demonstration of the metabolic consequences of these pathogenic antibodies during obesity. In summary, the present study raises the prospect of targeting T-bet^{+} B cells in future therapeutic approaches to limit metabolic disorder and reverse symptoms of T2D, and potentially other inflammatory disorders.

LIMITATIONS OF STUDY

These studies identify a key contribution of Tbet+ B cell-derived IgG to inflammation during obesity. While antibodies produced by Tbet+ B cells in other contexts have been characterized as autoimmune, and this is also a likely scenario during obesity, this study does not determine the specificity of IgG2c Abs. The nature of epitopes targeted by adipose Tbet+ B cells remain a very compelling question with broad implications for obesity, T2D, and all sterile inflammatory conditions.

The potential for Tbet+ B cells to recognize local adipose-derived antigens also raises the question of the source and location of T cell help for Tbet+ B cells. Tbet+ B cells likely receive an activating signal through TLR 7 or TLR 9, but still require a second helper signal

from T cells to survive and produce their antibodies (Cancro, 2020). It is likely Tbet+ B cells receive supporting cytokines or co-stimulation from helper iNKT$_{FH}$, T$_{FH,}$ and/or T$_{PH}$ cells, but this remains to be shown. While recent studies suggest TLR7-driven autoimmunity by similar human DN2 or Age Associated B cells (ABCs) is GC-independent (Brown et al., 2022), it remains to be determined if classs-witched adipose IgG2c-producing Tbet+ B cells receive their T cell help via a GC or extra-follicular interactions. Non-resident adipose ABCs were previously shown to be expanded in fat associated lymphoid clusters during aging as a consequence of IL-1 signaling through the NLRP3 inflammasome (Camell et al., 2019), suggesting another possible mechanism for Tbet+ B cell expansion during obesity. These studies also did not localize Tbet+ B cells within the spleen or adipose tissue nor determine whether they are activated and helped in separate locations.

Obesity is often described as inducing a form of accelerated aging (Fulop et al., 2021). This study does not comprehensively distinguish between the two, beyond determining that Tbet+ B cell increases in adipose tissue correlated with weight/BMI but not age in this cohort of patients. Indeed, this finding may reflect the advanced nature of disease in the patients and mice with obesity in these studies.

STAR Methods

RESOURCE AVAILABILITY

Lead contact—Further information and requests for resources and reagents will be fulfilled by the Lead Contact, Elizabeth A. Leadbetter (leadbetter@uthscsa.edu).

Materials availability—Material and resources essential to reproduce results presented in the manuscript are detailed in the Key Resources Table. Unique mice bred for this study will be made available by the Lead Contact.

Data and Code Availability

- All data reported in this paper can be found in the associated file, “Data S1-Source Data”, or will be shared by the lead contact upon request.
- This paper does not report original code.
- Any additional information required to reanalyze the data reported in this paper is available from the lead contact upon request.

EXPERIMENTAL MODELS AND SUBJECT DETAILS

Human Subjects—Resected dermal tissue with attached subcutaneous adipose tissue was obtained from lean, overweight, and obese female subjects who underwent plastic surgery at the San Antonio Plastic Surgery Institute at the Christus Santa Rosa Hospital, San Antonio, USA. 17 obese patients (mean age 42, range 40–50; mean BMI 32), 22 overweight (mean age 42, range 40–50; mean BMI 32), and 10 lean (mean age 42, range 40–50; mean BMI 32) patients following a range of different elective plastic surgery procedures but predominantly abdominoplasty. All patient samples were obtained under an IRB exception

approved by the UT Health ethics committee. Further information about the cohort and subject characteristics is detailed in Table S1 of the manuscript.

Mice—C57BL/6J wild-type mice (#000664), B6.129P2(C)-*Cd19*$^{tm1(cre)Cgn}$/J (#006785), and congenic B6.129S4-CXCL10^{tm1Adl}/J (#006087)(Dufour et al., 2002) were obtained from The Jackson Laboratory. B6.129-*Tbx21*^{tm2Srnr}/J mice (Jax#022741) were obtained from N. Zhang (UT Health). *Cd19*$^{Cre/+}$ and *Tbx21*$^{flox/flox}$ mice were intercrossed to generate *Tbx21*$^{flox/flox}$ *Cd19*$^{Cre/+}$ and *Tbx21*$^{flox/flox}$ *Cd19*$^{Cre/Cre}$ mice. iNKT cell-deficient B6.129S6-Del(3Cd1d2-Cd1d1)1Sbp/J mice (Sonoda et al., 1999) (#008881) were obtained from M. Exley (University of Manchester, UK) while B6.Jα18−/− mice (Cui et al., 1997) were obtained from M. Brenner (Brigham and Women's Hospital/Harvard Medical School). B6.129P2(C)-*Igh*^{tm2Cgn}/J (#012642) B6.SJL B1–8^{hi} mice heterozygous for targeted insertion of a high affinity mutated variable 186.2 immunoglobulin heavy chain bearing specificity for the hapten NP(Shih et al., 2002) were provided by M. Nussenzweig (Rockefeller University), C57BL/6 Valpha14-transgenic mice with an increased frequency of iNKT cells (Bendelac et al., 1996) were provided by M. Brenner (Brigham and Women's Hospital/Harvard School of Medicine). C.129S4(B6)-*Ifng*$^{tm3.1Lky}$/J (GREAT) IFN gamma reporter mice (JAX #017580) were provided by M. Mohrs (Trudeau Institute). All mice were housed and bred under specific pathogen-free conditions at the animal facility of UT Health (UTHSCSA).

Age- and sex-matched female or male mice 6–24 weeks of age were used in all experiments. All mice were maintained in individually ventilated cages. Up to five mice per cage were housed in individually ventilated cages in a 12 hour light/dark cycle, with room temperature at 22 C (19 C-23 C change). They were fed with autoclaved standard pellet chow or high-fat chow (Research Diets) and water *ad libitum*. Experimental mice and littermate controls for obesity studies were initiated on the high fat chow (HFD) between 6–8 weeks of age and maintained on the diet for 8–15 weeks. Bedding was exchanged between all cages 1 week prior to initiation of HFD. Mice were weighed bi-weekly and their health monitored closely. 2 to 5 mice were used per experimental group, including age and sex matched cage mate or littermate controls. All mice were randomly assigned to experimental treatment groups. All experiments were performed under UT Health Animal Care and Use Committee- approved protocols.

METHOD DETAILS

Murine Tissues—Peri-epididymal white adipose tissue was dissected and minced with fine scissors. Minced adipose tissue was digested with collagenase (Sigma-Aldrich, 0.1 mg per ml) in RPMI for 30 min at 37°C on a belly dancer shaker. Following digestion, supernatants were filtered through 100 um cell strainers and pelleted by centrifugation. Cell yields and viability were measured by trypan blue and a hemocytometer. Spleens were dissected and forced through a 100 um metal strainer to generate a single cell suspension before red blood cells were lysed using ACK buffer.

PCR—DNA was isolated from tail snips, B lymphocytes negatively selected, or non-B cells retained on the column from EasySep™ Mouse B cell isolation kit (Cat# 19854, Stemcell

Technologies) using proteinase K-containing lysis buffer. Supernatant containing genomic DNA (gDNA) was precipitated using alcohol, and then gDNA was resuspended in TE buffer. gDNA from C57BL/6 wild-type, splenic B cells and splenic non-B cells were used as a template to amplify the *Tbx21* (Tbet) gene. PCR master mix consisted of dNTPs, PCR buffer, $MgCl_2$, Taq Polymerase (Thermo Fisher, Catalog# 10-966-026) with the following primers: Forward primer: 5'-AACTGTGTTCCCGAGGTGTC-3'. Reverse primer: 5'-GGAGCCCACAAGCCATTACA-3'. After 35cycles of amplification, the expected product length is 2875 bp.

Human Tissues—Following procurement of resected skin along with attached subcutaneous fat, adipose tissue was removed and minced using scissors. DPBS (Hyclone) with collagenase IV (Sigma) corresponding to half the volume of minced tissue was added to the tissue to yield a final concentration of 200 mg/ml collagenase for the tissue suspension. Minced adipose tissue was incubated at 37°C for 1h on a BellyDancer shaker. Following digestion, tissue supernatant was transferred to 50 ml conical tubes and centrifuged at 2400 rpm at room temperature. Pellets containing cells were extracted and washed twice followed by red blood cell lysis at room temperature in 15 ml ACK for 10 min. The cells were then washed twice and filtered through a 40 um nylon mesh, followed by cell counting and processing for flow cytometry.

Injections, Diet, and Metabolic Studies—C57BL/6 mice were given intraperitoneal injection of 50 μg Resiquimod (R848, Invitrogen) on day 0 and 50 μg Resiquimod on day 2 or 3. B1–8^{hi} mice were given intraperitoneal injection of 50 μg Resiquimod (R848, Invitrogen) on day 0 and 50 μg Resiquimod plus 100 μg NP-KLH on day 2 or 3. The mice were sacrificed and spleens were collected for analysis and/or transfer on day 4 (as noted in the figure legends).

Where indicated, mice were provided with either normal chow diet (NCD) or high fat diet (HFD) (Research Diets, 60 kcal% fat) *ad libitum* and weighed at least one time per week. Whole abdominal adipose fat pads were weighed after dissection. After no less than 6 weeks on HFD, fasting blood glucose was measured (OneTouch Ultra). For glucose tolerance tests, fasted (6 hr) mice received 1 g glucose per kg body weight intraperitoneally, and glucose levels were measured every 15 min for up to 180 min.

Lymphocyte isolation and adoptive transfers—For adoptive transfer of B cells, splenocytes in single-cell suspensions were harvested from I or R848/NP-KLH-injected (8–12 week old) lean B6.SJL B1–8^{hi} mice on day 4 as noted in figure legends. In some experiments, wild-type mice were injected with R848 only prior to B cell harvest. B cells were negatively selected using the EasySep™ B Cell Isolation Kit (Stemcell Technologies) according to manufacturer's instructions. This kit does not include anti-CD11c, so Tbet+ CD11c+ B cells remained in the negative selection population. Post-enrichment cells were then analyzed by flow cytometry using a BD FACS Celesta (Becton Dickinson, >95% purity). 10^7 cells were then transferred to naïve wild-type recipients fed NCD or HFD via intravenous or intraperitoneal injection, as noted in figure legends. Preliminary testing confirmed the clear presence of CD45.1+ congenically marked, transferred B cells in

recipient mice 5 days post transfer (see Figure S5B) at frequencies proportional to the number of cells transferred.

Serum for adoptive transfer was collected by submandibular terminal bleed from WT mice fed a HFD for 12+ weeks. Sample was pooled from 10 mice, stored −80C before transfer of 150ul/mouse via i.p. injection. Purified IgG for adoptive transfer was isolated from serum collected from 10 WT mice fed a HFD for 12+ weeks. Total IgG was isolated from serum passaged over a Melon™ Gel IgG Spin Purification column (Cat#45206, ThermoFisher). The flow-through from the columns containing the IgG antibodies was dialyzed with sterile PBS using Pierce™ Protein Concentrators PES, 50K MWCO (Cat#88538, Thermo Scientific). IgM, IgG, and IgG2c concentrations were confirmed by ELISA prior to transfer. 150uL of sterile PBS containing–179 – 257ug IgG antibodies were transferred to recipient mice on Day 0 and Day 3. GTTs were performed at Day 7.

Mixed Bone-Marrow Chimeras—Recipient *Cd19*$^{Cre/+}$ and *Tbx21*$^{flox/flox}$ mice were irradiated with a total of 900 rads distributed over two occasions and were allowed to rest for a few hours followed by bone marrow reconstitution. Recipient mice were reconstituted with 5×10^6 bone marrow cells and rested for at least 9 weeks. Donor bone marrow included either 75% *Cd19*$^{Cre/+}$ and *Tbx21*$^{flox/flox}$ bone marrow mixed with 25% CXCL10−/− bone marrow, or 75% *Cd19*$^{Cre/+}$ and *Tbx21*$^{flox/flox}$ bone marrow mixed with 25% WT CXCL10+/+ bone marrow. These reconstitution mixtures resulted in mice in which only the Tbet+ B cells were deficient in CXCL10 expression or all cells were CXCL10 sufficient. Graft reconstitution was evaluated by WAT and spleen analysis of CD45.1+ congenic markers expressed by donor CXCL10−/− or CXCL10+/+ lymphocytes.

In vitro assays—Splenocytes in single-cell suspensions were harvested from naive C57BL/6 wild-type mice. 1.5×10^5 total splenocytes or isolated B cells were plated in 96-well flat-bottomed plates and cultured in complete RPMI with 10% FCS in vitro for 48 h in the absence or presence of 2.5 ug/ml of Resiquimod (R848) followed by analysis by flow cytometry. B cells were negatively selected using the EasySep™ B Cell Isolation Kit (Stemcell Technologies) according to the manufacturer's instructions. Supernatants were collected and stored at minus 80°C until assessment by ELISA.

ELISA—Serum was isolated from blood collected via the tail or submandibular vein, and samples were stored at minus 20°C until assessment by ELISA. Anti-H+L chain capturing antibody was used (Southern Biotech) and all antibodies were detected with HRP-conjugated secondary anti-mouse IgG1, IgG2c, and IgG3 (Southern Biotech). 2,2′-Azino-bis(3-ethylbenzthiazoline-6-sulfonic acid) (ABTS) substrate (Millipore-Sigma) was used as a substrate for the HRP enzyme. CXCL10 in sera was measured by solid phase sandwich ELISA using the Mouse DuoSet ELISA kit (R&D Systems) according to the manufacturer's instructions.

Flow Cytometry—Fc receptors on splenocytes in single-cell suspension were blocked with purified anti-mouse CD16/32 (Bio × Cell) to reduce non-specific labeling, and the cells were stained with Live/Dead Fixable Aqua viability dye (Life Technologies) for 10 minutes at room temperature. Cells were then washed and stained using indicated antibodies

(BD Pharmingen, Biolegend, R&D Systems, or eBiosciences) for 30 minutes on ice. iNKT cells were identified with tetramers of PBS57-loaded CD1d tetramer (kindly provided by the NIH tetramer core facility) conjugated to allophycocyanin, phycoerythrin, or Brilliant Violet 421™. For intracellular staining of cytokines or transcription factors, cells were processed using the Foxp3 staining kit (eBioscience) according to the manufacturer's instructions. Finally, cells were resuspended in FACS buffer and analyzed on a Celesta cytometer (BD Biosciences). Doublet exclusion and live-cell discrimination was performed on all cell populations prior to further subgating. Between 5×10^5 and 1×10^7 events were collected for extracellular stained samples and 5.0×10^5 events for samples stained for intracellular markers. For *in vitro* cultures, all cells present in culture dishes were analyzed. Samples were analyzed using FlowJo software (TreeStar) or Diva software (BD Biosciences).

Histological Staining and Digital Imaging Analysis—Livers were perfused, then liver or adipose tissue was collected from *Cd19*$^{Cre/+}$ and *Tbx21*$^{flox/flox}$ or littermate controls and immediately snap frozen in OCT (Tissue-Tek). Hepatic steatosis was examined by Oil Red O dye, a Sudan stain specific for lipids. Adipocyte diameter was assessed by H & E staining. Frozen tissue samples were sliced into 12μm sections with a Cryostat at −18°C. There were two to four slides sectioned from each mouse. Slides were examined and imaged with Brightfield by Zeiss Microscope in the UTHealth MIMG Department Microscope Facility. For Oil Red O-stained livers, five images were collected per slide beginning at the portal vein and the right, bottom, left, and top of the portal vein image. Lipid staining in five images per section, 2–4 sections per mouse was quantified using FIJI software to determine the pixels of area covered by lipid deposit (red staining above a common baseline threshold set for all images from one experiment) as a ratio of the total area of the image (% area). Images were confirmed to have the same total area in pixels. For adipocyte diameter, circumference of 5 cells per section, 2–4 sections per mouse of H & E labeled adipose tissue were outlined and used to calculate average cell diameters per section by Fiji software.

QUANTIFICATION AND STATISTICAL ANALYSIS

Statistical significance was assessed with a two-tailed Student's *t*-test, paired *t*-test, or 1-way ANOVA, as indicated in figure legends. Sample size was chosen based on previous studies when statistical significance was achieved. *P* values of less than 0.05 were considered statistically significant and marked with an asterisk as noted in figure legends. Statistical analysis was performed using GraphPad PRISM 7 software. Box heights and symbol centers indicate group means and/or individual values. Error bars indicate s.e.m. Where indicated, the tSNE algorithm was used to visualize data obtained from flow cytometry using FlowJo (TreeStar).

Supplementary Material

Refer to Web version on PubMed Central for supplementary material.

ACKNOWLEDGEMENTS

We thank L. Lynch (Harvard Medical School/Trinity College Dublin), E. Meffre (Yale School of Medicine), G. Winslow (SUNY Upstate Medical University), and M. Jenkins (University of Minnesota Medical School) for fruitful discussions and kind assistance. We thank the UT Health Flow Cytometry Core and vivarium for essential

services and the US NIH Tetramer Core for CD1d-PBS57 tetramers. We are indebted to Dr. Michael Decherd, Kim Arnold, and the patients of the San Antonio Plastic Surgery Institute for essential clinical samples. We thank M. Nussenzweig (Rockefeller University), M. Exley (University of Manchester, UK), M. Mohrs (Trudeau Institute), and M. Brenner (BWH/HMS) for critical mouse strains. This study was supported by the Swedish Research Council (T.H.), NIH R01 AI32798-01A1 (EAL), a Voelcker Fund Young Investigator Award (EAL), and UT Health faculty support (EAL).

REFERENCES

Agrawal S, and Gupta S (2011). TLR1/2, TLR7, and TLR9 signals directly activate human peripheral blood naive and memory B cell subsets to produce cytokines, chemokines, and hematopoietic growth factors. J Clin Immunol 31, 89–98. [PubMed: 20821041]

Ashouri JF, and Weiss A (2017). Endogenous Nur77 Is a Specific Indicator of Antigen Receptor Signaling in Human T and B Cells. J Immunol 198, 657–668. [PubMed: 27940659]

Bapat SP, Myoung Suh J, Fang S, Liu S, Zhang Y, Cheng A, Zhou C, Liang Y, LeBlanc M, Liddle C, et al. (2015). Depletion of fat-resident Treg cells prevents age-associated insulin resistance. Nature 528, 137–141. [PubMed: 26580014]

Barnett BE, Staupe RP, Odorizzi PM, Palko O, Tomov VT, Mahan AE, Gunn B, Chen D, Paley MA, Alter G, et al. (2016). Cutting Edge: B Cell-Intrinsic T-bet Expression Is Required To Control Chronic Viral Infection. J Immunol 197, 1017–1022. [PubMed: 27430722]

Bendelac A, Hunziker RD, and Lantz O (1996). Increased interleukin 4 and immunoglobulin E production in transgenic mice overexpressing NK1 T cells. J Exp Med 184, 1285–1293. [PubMed: 8879200]

Brown GJ, Canete PF, Wang H, Medhavy A, Bones J, Roco JA, He Y, Qin Y, Cappello J, Ellyard JI, et al. (2022). TLR7 gain-of-function genetic variation causes human lupus. Nature 605, 349–356. [PubMed: 35477763]

Camell CD, Gunther P, Lee A, Goldberg EL, Spadaro O, Youm YH, Bartke A, Hubbard GB, Ikeno Y, Ruddle NH, et al. (2019). Aging Induces an Nlrp3 Inflammasome-Dependent Expansion of Adipose B Cells That Impairs Metabolic Homeostasis. Cell Metab 30, 1024–1039 e1026. [PubMed: 31735593]

Cancro MP (2020). Age-Associated B Cells. Annu Rev Immunol 38, 315–340. [PubMed: 31986068]

Chawla A, Nguyen KD, and Goh YP (2011). Macrophage-mediated inflammation in metabolic disease. Nat Rev Immunol 11, 738–749. [PubMed: 21984069]

Cui J, Shin T, Kawano T, Sato H, Kondo E, Toura I, Kaneko Y, Koseki H, Kanno M, and Taniguchi M (1997). Requirement for Valpha14 NKT cells in IL-12-mediated rejection of tumors. Science 278, 1623–1626. [PubMed: 9374462]

Dufour JH, Dziejman M, Liu MT, Leung JH, Lane TE, and Luster AD (2002). IFN-gamma-inducible protein 10 (IP-10; CXCL10)-deficient mice reveal a role for IP-10 in effector T cell generation and trafficking. J Immunol 168, 3195–3204. [PubMed: 11907072]

Ehrhardt GR, Hsu JT, Gartland L, Leu CM, Zhang S, Davis RS, and Cooper MD (2005). Expression of the immunoregulatory molecule FcRH4 defines a distinctive tissue-based population of memory B cells. J Exp Med 202, 783–791. [PubMed: 16157685]

Enoksson SL, Grasset EK, Hagglof T, Mattsson N, Kaiser Y, Gabrielsson S, McGaha TL, Scheynius A, and Karlsson MC (2011). The inflammatory cytokine IL-18 induces self-reactive innate antibody responses regulated by natural killer T cells. Proc Natl Acad Sci U S A 108, E1399–1407. [PubMed: 22135456]

Frasca D, Diaz A, Romero M, and Blomberg BB (2021). Phenotypic and Functional Characterization of Double Negative B Cells in the Blood of Individuals With Obesity. Front Immunol 12, 616650. [PubMed: 33708209]

Fulop T, Larbi A, Pawelec G, Khalil A, Cohen AA, Hirokawa K, Witkowski JM, and Franceschi C (2021). Immunology of Aging: the Birth of Inflammaging. Clin Rev Allergy Immunol.

Grela F, Aumeunier A, Bardel E, Van LP, Bourgeois E, Vanoirbeek J, Leite-de-Moraes M, Schneider E, Dy M, Herbelin A, et al. (2011). The TLR7 agonist R848 alleviates allergic inflammation by targeting invariant NKT cells to produce IFN-gamma. J Immunol 186, 284–290. [PubMed: 21131420]

Guerendiain M, Montes R, Lopez-Belmonte G, Martin-Matillas M, Castellote AI, Martin-Bautista E, Marti A, Martinez JA, Moreno L, Garagorri JM, et al. (2018). Changes in plasma fatty acid composition are associated with improvements in obesity and related metabolic disorders: A therapeutic approach to overweight adolescents. Clinical nutrition (Edinburgh, Scotland) 37, 149–156.

Hagglof T, Sedimbi SK, Yates JL, Parsa R, Salas BH, Harris RA, Leadbetter EA, and Karlsson MC (2016). Neutrophils license iNKT cells to regulate self-reactive mouse B cell responses. Nat Immunol 17, 1407–1414. [PubMed: 27798616]

Hanna Kazazian N, Wang Y, Roussel-Queval A, Marcadet L, Chasson L, Laprie C, Desnues B, Charaix J, Irla M, and Alexopoulou L (2019). Lupus Autoimmunity and Metabolic Parameters Are Exacerbated Upon High Fat Diet-Induced Obesity Due to TLR7 Signaling. Front Immunol 10, 2015. [PubMed: 31552019]

Hao Y, O'Neill P, Naradikian MS, Scholz JL, and Cancro MP (2011). A B-cell subset uniquely responsive to innate stimuli accumulates in aged mice. Blood 118, 1294–1304. [PubMed: 21562046]

Harmon DB, Srikakulapu P, Kaplan JL, Oldham SN, McSkimming C, Garmey JC, Perry HM, Kirby JL, Prohaska TA, Gonen A, et al. (2016). Protective Role for B-1b B Cells and IgM in Obesity-Associated Inflammation, Glucose Intolerance, and Insulin Resistance. Arterioscler Thromb Vasc Biol 36, 682–691. [PubMed: 26868208]

Intlekofer AM, Banerjee A, Takemoto N, Gordon SM, Dejong CS, Shin H, Hunter CA, Wherry EJ, Lindsten T, and Reiner SL (2008). Anomalous type 17 response to viral infection by CD8+ T cells lacking T-bet and eomesodermin. Science 321, 408–411. [PubMed: 18635804]

Isnardi I, Ng YS, Menard L, Meyers G, Saadoun D, Srdanovic I, Samuels J, Berman J, Buckner JH, Cunningham-Rundles C, et al. (2010). Complement receptor 2/CD21- human naive B cells contain mostly autoreactive unresponsive clones. Blood 115, 5026–5036. [PubMed: 20231422]

Kenderes KJ, Levack RC, Papillion AM, Cabrera-Martinez B, Dishaw LM, and Winslow GM (2018). T-Bet(+) IgM Memory Cells Generate Multi-lineage Effector B Cells. Cell Rep 24, 824–837 e823. [PubMed: 30044980]

King IL, Fortier A, Tighe M, Dibble J, Watts GF, Veerapen N, Haberman AM, Besra GS, Mohrs M, Brenner MB, et al. (2011). Invariant natural killer T cells direct B cell responses to cognate lipid antigen in an IL-21-dependent manner. Nat Immunol 13, 44–50. [PubMed: 22120118]

Kohlgruber AC, Donado CA, LaMarche NM, Brenner MB, and Brennan PJ (2016). Activation strategies for invariant natural killer T cells. Immunogenetics 68, 649–663. [PubMed: 27457886]

LaMarche NM, Kane H, Kohlgruber AC, Dong H, Lynch L, and Brenner MB (2020). Distinct iNKT Cell Populations Use IFNgamma or ER Stress-Induced IL-10 to Control Adipose Tissue Homeostasis. Cell Metab 32, 243–258 e246. [PubMed: 32516575]

Leadbetter EA, Brigl M, Illarionov P, Cohen N, Luteran MC, Pillai S, Besra GS, and Brenner MB (2008). NK T cells provide lipid antigen-specific cognate help for B cells. Proc Natl Acad Sci U S A 105, 8339–8344. [PubMed: 18550809]

Lee JY, Zhao L, Youn HS, Weatherill AR, Tapping R, Feng L, Lee WH, Fitzgerald KA, and Hwang DH (2004). Saturated fatty acid activates but polyunsaturated fatty acid inhibits Toll-like receptor 2 dimerized with Toll-like receptor 6 or 1. J Biol Chem 279, 16971–16979. [PubMed: 14966134]

Lynch L (2014). Adipose invariant natural killer T cells. Immunology 142, 337–346. [PubMed: 24673647]

Lynch L, Nowak M, Varghese B, Clark J, Hogan AE, Toxavidis V, Balk SP, O'Shea D, O'Farrelly C, and Exley MA (2012). Adipose tissue invariant NKT cells protect against diet-induced obesity and metabolic disorder through regulatory cytokine production. Immunity 37, 574–587. [PubMed: 22981538]

Lynch L, O'Shea D, Winter DC, Geoghegan J, Doherty DG, and O'Farrelly C (2009). Invariant NKT cells and CD1d(+) cells amass in human omentum and are depleted in patients with cancer and obesity. Eur J Immunol 39, 1893–1901. [PubMed: 19585513]

Manni M, Gupta S, Ricker E, Chinenov Y, Park SH, Shi M, Pannellini T, Jessberger R, Ivashkiv LB, and Pernis AB (2018). Regulation of age-associated B cells by IRF5 in systemic autoimmunity. Nat Immunol 19, 407–419. [PubMed: 29483597]

Mathis D (2013). Immunological goings-on in visceral adipose tissue. Cell Metab 17, 851–859. [PubMed: 23747244]

Moir S, Ho J, Malaspina A, Wang W, DiPoto AC, O'Shea MA, Roby G, Kottilil S, Arthos J, Proschan MA, et al. (2008). Evidence for HIV-associated B cell exhaustion in a dysfunctional memory B cell compartment in HIV-infected viremic individuals. J Exp Med 205, 1797–1805. [PubMed: 18625747]

Naradikian MS, Myles A, Beiting DP, Roberts KJ, Dawson L, Herati RS, Bengsch B, Linderman SL, Stelekati E, Spolski R, et al. (2016). Cutting Edge: IL-4, IL-21, and IFN-gamma Interact To Govern T-bet and CD11c Expression in TLR-Activated B Cells. J Immunol 197, 1023–1028. [PubMed: 27430719]

Nishimura S, Manabe I, Takaki S, Nagasaki M, Otsu M, Yamashita H, Sugita J, Yoshimura K, Eto K, Komuro I, et al. (2013). Adipose Natural Regulatory B Cells Negatively Control Adipose Tissue Inflammation. Cell Metab.

Osborn O, and Olefsky JM (2012). The cellular and signaling networks linking the immune system and metabolism in disease. Nat Med 18, 363–374. [PubMed: 22395709]

Peng SL, Szabo SJ, and Glimcher LH (2002). T-bet regulates IgG class switching and pathogenic autoantibody production. Proc Natl Acad Sci U S A 99, 5545–5550. [PubMed: 11960012]

Reinhardt RL, Liang HE, and Locksley RM (2009). Cytokine-secreting follicular T cells shape the antibody repertoire. Nat Immunol 10, 385–393. [PubMed: 19252490]

Rickert RC, Roes J, and Rajewsky K (1997). B lymphocyte-specific, Cre-mediated mutagenesis in mice. Nucleic acids research 25, 1317–1318. [PubMed: 9092650]

Rubtsov AV, Rubtsova K, Fischer A, Meehan RT, Gillis JZ, Kappler JW, and Marrack P (2011). Toll-like receptor 7 (TLR7)-driven accumulation of a novel CD11c(+) B-cell population is important for the development of autoimmunity. Blood 118, 1305–1315. [PubMed: 21543762]

Rubtsova K, Rubtsov AV, Thurman JM, Mennona JM, Kappler JW, and Marrack P (2017). B cells expressing the transcription factor T-bet drive lupus-like autoimmunity. J Clin Invest 127, 1392–1404. [PubMed: 28240602]

Rubtsova K, Rubtsov AV, van Dyk LF, Kappler JW, and Marrack P (2013). T-box transcription factor T-bet, a key player in a unique type of B-cell activation essential for effective viral clearance. Proc Natl Acad Sci U S A 110, E3216–3224. [PubMed: 23922396]

Schulthess FT, Paroni F, Sauter NS, Shu L, Ribaux P, Haataja L, Strieter RM, Oberholzer J, King CC, and Maedler K (2009). CXCL10 impairs beta cell function and viability in diabetes through TLR4 signaling. Cell Metab 9, 125–139. [PubMed: 19187771]

Shen L, Chng MH, Alonso MN, Yuan R, Winer DA, and Engleman EG (2015). B-1a lymphocytes attenuate insulin resistance. Diabetes 64, 593–603. [PubMed: 25249575]

Shih TA, Roederer M, and Nussenzweig MC (2002). Role of antigen receptor affinity in T cellindependent antibody responses in vivo. Nat Immunol 3, 399–406. [PubMed: 11896394]

Sonoda KH, Exley M, Snapper S, Balk SP, and Stein-Streilein J (1999). CD1-reactive natural killer T cells are required for development of systemic tolerance through an immune-privileged site. J Exp Med 190, 1215–1226. [PubMed: 10544194]

Szabo SJ, Kim ST, Costa GL, Zhang X, Fathman CG, and Glimcher LH (2000). A novel transcription factor, T-bet, directs Th1 lineage commitment. Cell 100, 655–669. [PubMed: 10761931]

Tomita K, Freeman BL, Bronk SF, LeBrasseur NK, White TA, Hirsova P, and Ibrahim SH (2016). CXCL10-Mediates Macrophage, but not Other Innate Immune Cells-Associated Inflammation in Murine Nonalcoholic Steatohepatitis. Sci Rep 6, 28786. [PubMed: 27349927]

van der Maaten LJP, and Hinton GE (2008). Visualizing High-Dimensional Data Using t-SNE. Journal of Machine Learning Research 9, 2579–2605.

Van LP, Bardel E, Gregoire S, Vanoirbeek J, Schneider E, Dy M, and Thieblemont N (2011). Treatment with the TLR7 agonist R848 induces regulatory T-cell-mediated suppression of established asthma symptoms. Eur J Immunol 41, 1992–1999. [PubMed: 21480211]

Vomhof-DeKrey EE, Yates J, Hagglof T, Lanthier P, Amiel E, Veerapen N, Besra GS, Karlsson MC, and Leadbetter EA (2015). Cognate interaction with iNKT cells expands IL-10-producing B regulatory cells. Proc Natl Acad Sci U S A 112, 12474–12479. [PubMed: 26392556]

Wang S, Wang J, Kumar V, Karnell JL, Naiman B, Gross PS, Rahman S, Zerrouki K, Hanna R, Morehouse C, et al. (2018). IL-21 drives expansion and plasma cell differentiation of autoreactive CD11c(hi)T-bet(+) B cells in SLE. Nature communications 9, 1758.

Weisberg SP, McCann D, Desai M, Rosenbaum M, Leibel RL, and Ferrante AW Jr. (2003). Obesity is associated with macrophage accumulation in adipose tissue. The Journal of Clinical Investigation 112, 1796–1808. [PubMed: 14679176]

Weiss GE, Crompton PD, Li S, Walsh LA, Moir S, Traore B, Kayentao K, Ongoiba A, Doumbo OK, and Pierce SK (2009). Atypical memory B cells are greatly expanded in individuals living in a malaria-endemic area. J Immunol 183, 2176–2182. [PubMed: 19592645]

Winer DA, Winer S, Shen L, Wadia PP, Yantha J, Paltser G, Tsui H, Wu P, Davidson MG, Alonso MN, et al. (2011). B cells promote insulin resistance through modulation of T cells and production of pathogenic IgG antibodies. Nat Med 17, 610–617. [PubMed: 21499269]

Winzell MS, and Ahren B (2004). The high-fat diet-fed mouse: a model for studying mechanisms and treatment of impaired glucose tolerance and type 2 diabetes. Diabetes 53 Suppl 3, S215–219. [PubMed: 15561913]

Wu L, Parekh VV, Hsiao J, Kitamura D, and Van Kaer L (2014). Spleen supports a pool of innate-like B cells in white adipose tissue that protects against obesity-associated insulin resistance. Proc Natl Acad Sci U S A 111, E4638–4647. [PubMed: 25313053]

Xu H, Barnes GT, Yang Q, Tan G, Yang D, Chou CJ, Sole J, Nichols A, Ross JS, Tartaglia LA, et al. (2003). Chronic inflammation in fat plays a crucial role in the development of obesity-related insulin resistance. J Clin Invest 112, 1821–1830. [PubMed: 14679177]

HIGHLIGHTS

- Activated Tbet+ B cells accumulate in adipose tissue of humans and mice with obesity
- iNKT cells support adipose accumulation and antibody production by Tbet+ B cells
- Mice lacking Tbet+ in B cells are protected from metabolic symptoms of obesity
- HFD-fed mouse IgG restores metabolic disease in obese mice lacking Tbet+ B cells

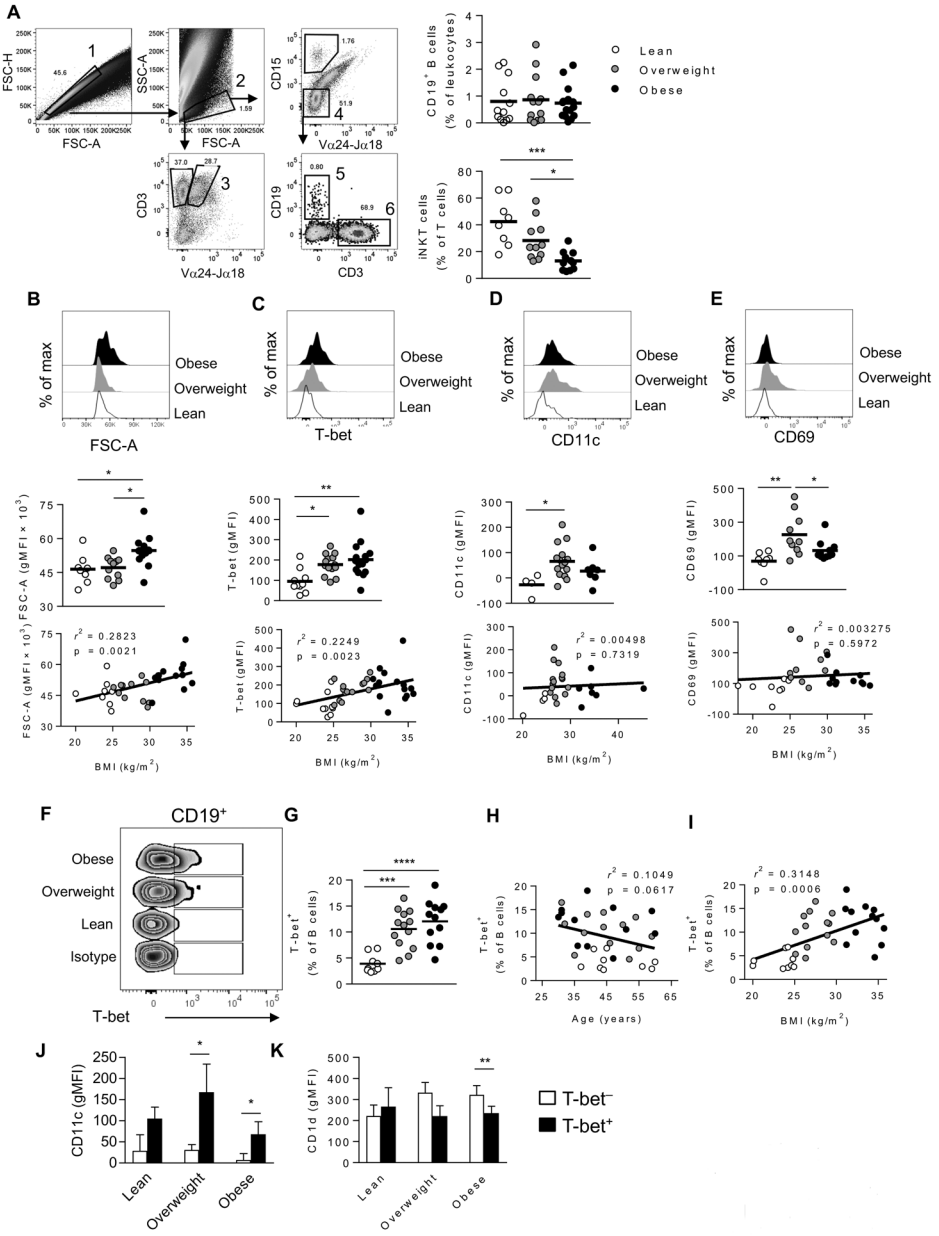

Figure 1. Increased expression of T-bet, CD11c, and CD69 in adipose B cells correlates with increasing BMI in humans with obesity.

(**A**) Flow cytometry plots display gating and frequency of B cells (gate 5) and iNKT cells (gate 3) in human subcutaneous adipose tissue. Dot plot quantifies B cell and iNKT cell frequency in adipose tissue from patients that are lean (white), overweight (gray), or obese (black); each dot represents one patient. (See also Table S1 and Figure S1). (**B-E**) Representative histograms, dot plot quantification, and correlation between body mass index (BMI; kg/m^2) of forward scatter-area (FSC-A) (**B**), intracellular T-bet protein expression (**C**), surface CD11c (**D**) and CD69 protein expression (**E**) for human adipose tissue B cells. Data are from >30 experiments. (**F**) Flow cytometry plot of CD19$^+$ cells and gating of T-bet$^+$ B cells from human adipose tissue. (**G**) Frequency of adipose tissue B cells that

are T-bet^{+}. Dots represent individual patients that are lean (white), overweight (gray), or obese (black). (H-I) Frequency of T-bet^{+} B cell correlation with patient age (H) or BMI (I). Quantification of CD11c (**J**) and CD1d protein expression (**K**) for T-bet^{-} (white) and T-bet^{+} (black) human adipose tissue B cells. (See also Figure S2) Dots represent one patient, line shows mean, bars indicate SEM; 1-way ANOVA. (**A**-**E**) Lines indicate linear regression trend with coefficient of determination (r^2); *p < 0.05, **p < 0.01, ***p < 0.001, ****p < 0.0001

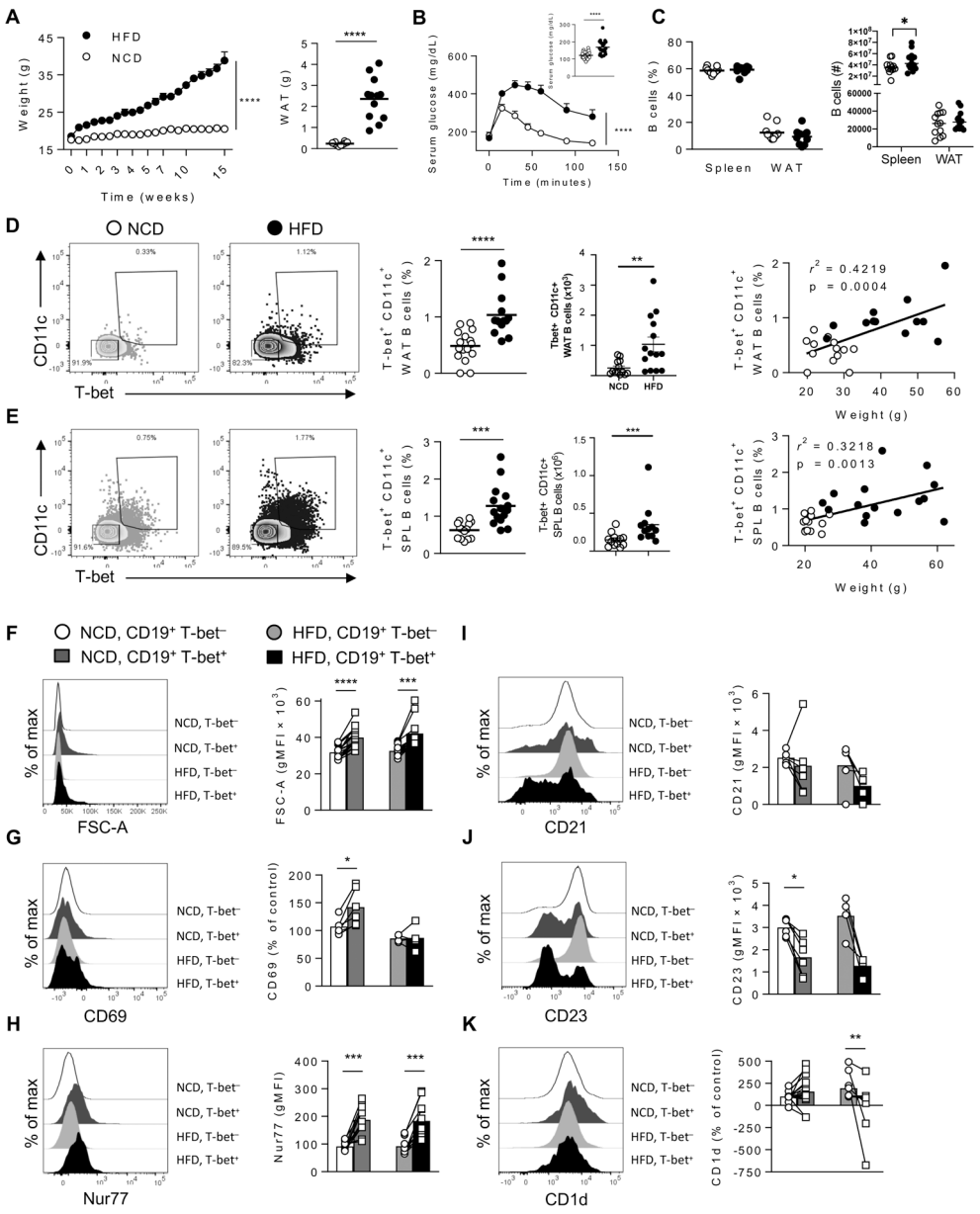

Figure 2. Murine adipose and splenic T-bet$^+$ B cell frequency and surface phenotype correlate with increasing body weight.

(**A**) Body weight and epididymal white adipose fat pad weight (week 15) of WT mice on the normal chow diet (NCD; white) or the high fat diet (HFD; black). (**B**) Glucose tolerance and resting serum glucose (week 15) measured by GTT. (**C**) Flow cytometry captures frequency and number of splenic and WAT CD19$^+$ B cells in WT. (**D**-**E**) Flow cytometry of B cells from adipose tissue (**D**) or spleen (**E**) of WT mice on the NCD or HFD. Zebra plots show gating of T-bet$^+$ CD11c$^+$ B cells, dot plots show frequency and number of T-bet$^+$ CD11c$^+$ cells from tissues indicated; correlation between frequency of tissue T-bet$^+$ CD11c$^+$ B cells and body weight. See also Figure S3. Representative histograms and quantification of FSC-A (**F**), CD69 (**G**), intracellular Nur77 protein (**H**), surface CD21 (**i**), CD23 (**j**), and

CD1d protein expression (**K**) for splenic $CD11c^{-}$ $T\text{-}bet^{-}$ B cells (circles; white, dark grey) and $T\text{-}bet^{+}$ $CD11c^{+}$ B cells (squares; light grey, black). Symbols represent one mouse on NCD (white, dark grey) or HFD (light grey, black). Data pooled from 4 (**A**-**B**), 2 (**C**), 7 (**D**-**E**), or 3 (**F**-**K**) experiments with 2–5 mice/grp and represented as mean ± SEM; 2way ANOVA, (**D**-**E**) Student's t-test; (**F**-**K**) Wilcoxon matched pairs signed-rank. (**D**-**E**) Lines indicate linear regression trend with coefficient of determination (r^2); *p < 0.05, **p < 0.01, ***p < 0.001, ****p < 0.0001.

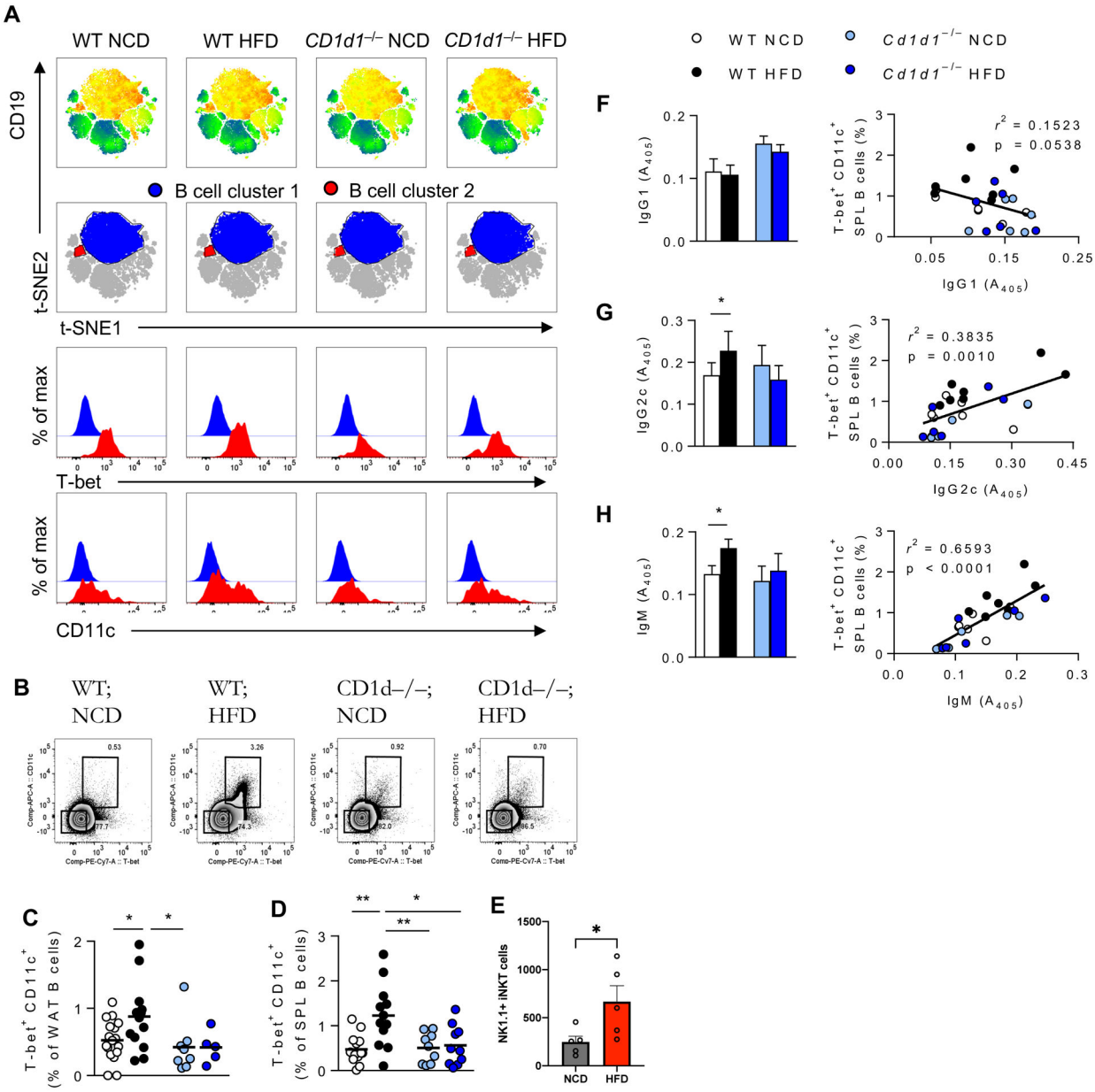

Figure 3. Expansion of T-bet$^+$ CD11c$^+$ B cells in diet-induced obesity depends on iNKT cells.

(**A**) Flow cytometry of lymphocytes from WT or *Cd1d1*$^{-/-}$ mice fed the NCD or HFD, presented with the t-SNE algorithm. See also Figure S4. Color in top row cell maps indicate expression of CD19: blue (low) to red (high). Second row cell maps indicate subgating of B cell cluster 1 (blue) and 2 (red). Histograms show expression of T-bet (third row) and CD11c (bottom row) by clusters identified in t-SNE maps; B cell cluster 1 (blue) and 2 (red). (**B-D**) Representative flow cytometry of splenic (**B**) and quantification of WAT and splenic (**C,D**) T-bet$^+$ CD11c$^+$ cell frequency of total B cells; WT NCD (white) and HFD (black), or *Cd1d1*$^{-/-}$ NCD (light blue) and HFD (dark blue). (**E**) Flow cytometric quantification of numbers of NK1.1+ iNKT cells in WAT from WT mice fed a NCD (grey) or HFD (red). (**F-G**) ELISA measure of serum IgG1 (**F**), IgG2c (**G**), and IgM (**H**) antibodies from WT

or *Cd1d1*$^{-/-}$ mice fed the NCD or HFD; correlation between frequency of splenic T-bet^{+} CD11c^{+} B cells and IgG1 (**F**), IgG2c (**G**), and IgM (**H**), assessed by flow cytometry and ELISA, respectively. WT NCD (white) and HFD (black), or *Cd1d1*$^{-/-}$ NCD (light blue) and HFD (dark blue). Dots represent individual mice. Data pooled from 7 (**A**-**D**), 2 (**E**), or 3 (**F**-**G**) experiments with at least 3 mice/grp. Mean ± SEM; (**B**-**C**) Two-way ANOVA; (**D**-**F**) Student's t-test and Student's paired t-test. Lines indicate linear regression trend with coefficient of determination (r^2); *p < 0.05, **p < 0.01, ***p < 0.001.

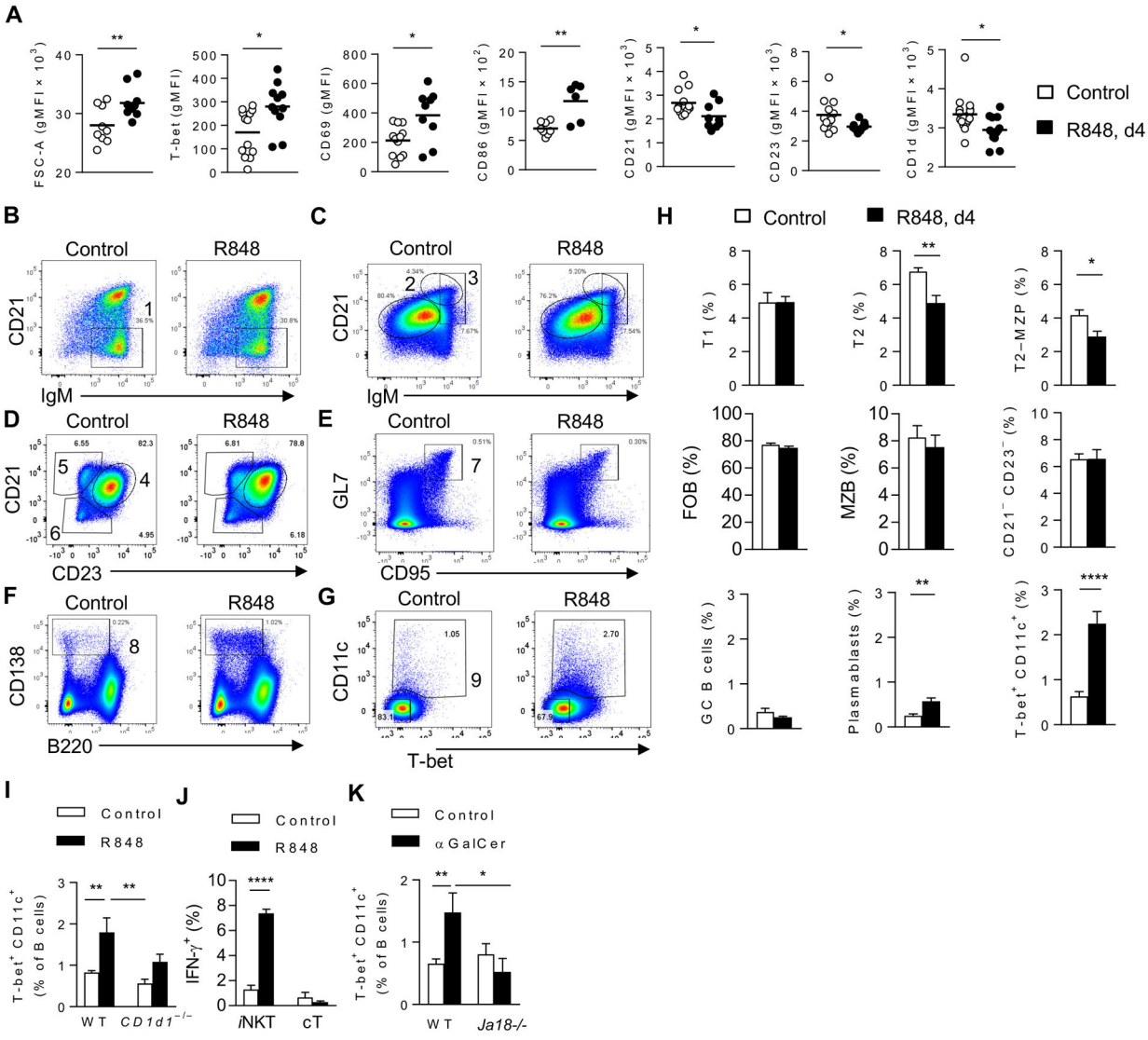

Figure 4. Innate signal-induced expansion of T-bet$^+$ CD11c$^+$ B cells is iNKT cell-dependent.

(**A**) Flow cytometry of FSC-A, intracellular T-bet protein, surface CD69, CD86, CD21, CD23, and CD1d protein expression for splenic CD19$^+$ B cells from WT mice administered 50μg R848 on day 0, 2 and harvested day 4 (black) or control (white). (**B-G**) Flow cytometry plots display gating strategy and frequency of B cell subsets in spleen of WT mice with (right) or without (left) R848 injection, as in (**A**). (**H**) Splenic B cell subset frequency from (**B-G**). Transitional type 1 (T1) gate 1, Transitional type 2 (T2) gate 2, Transitional type 2- Marginal zone precursor (T2-MZP) gate 3, Follicular B (FOB) gate 4, marginal zone B gate 5, CD21$^-$ CD23$^-$ gate 6, germinal center B (GC B) gate 7, plasmablast gate 8, CD11c$^+$ gate 9. (**I**) Flow cytometry quantification of Tbet$^+$ CD11c$^+$ B cell frequency, isolated from spleens harvested 4 days after injection of wild-type or *Cd1d1*$^{-/-}$ mice with (black) or without (white) R848. (**J**) Flow cytometry quantification of IFN-γ$^+$ cells among iNKT cells and conventional (c)T cells, isolated from spleens of GREAT C.129S4(B6)-*Ifng*$^{tm3.1Lky}$/J mice with (black) or without (white) R848 injection, harvested on day 4. (**K**) Flow cytometry of splenic T-bet$^+$ CD11c$^+$ B cells from wild-type

and *Jα18*$^{-/-}$ mice with (black) or without (white) i.p. injection of 0.5 μg αGalCer. Spleens were harvested 4 days after injection. Data are from at 3 (**A**, **I**-**J**, **N**), 2 (**B**-**H**), or 5 (**K**) experiments with at least 2 mice/grp. Dots represent one mouse and/or show mean ± SEM; bar height is mean ± SEM; (**A**-**H**) Student's t-test; (**I**-**K**) 1-way ANOVA. Line indicates linear regression trend with coefficient of determination (r^2); *p < 0.05, **p < 0.01, ***p < 0.001, ****p < 0.0001.

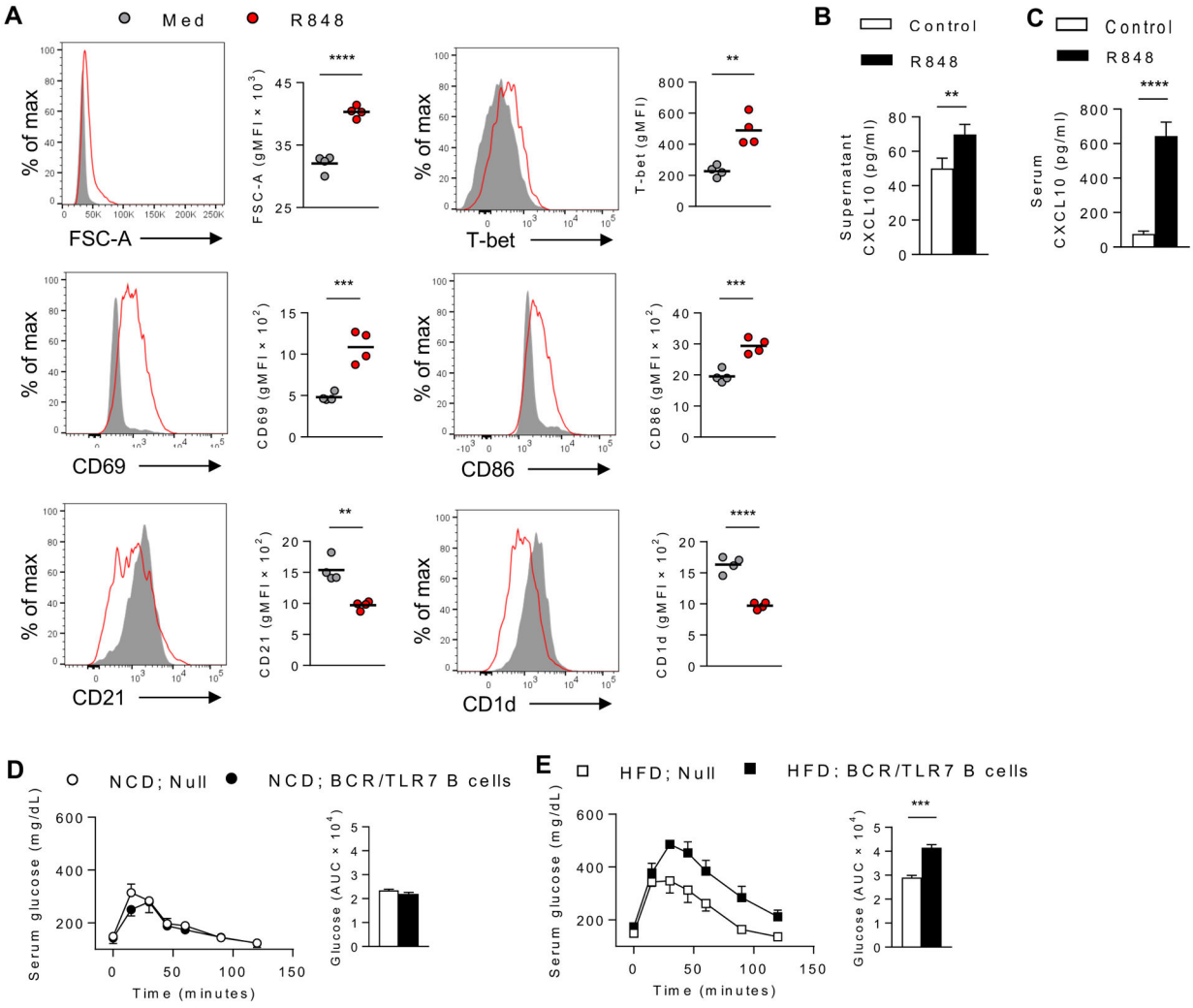

Figure 5. T-bet-expressing B cells secrete CXCL10 and contribute to metabolic disorder in obesity.

(**A**) Representative flow cytometry histograms and dot plot summaries of cell size (FSC-A), intracellular T-bet protein expression, surface CD69, CD86, CD21, and CD1d protein expression, of isolated WT splenic B cells cultured *in vitro* with (red dots/histograms) or without (gray dots/histograms) 2.5 μg/ml R848 for 48 hours. (**B**) ELISA quantification of CXCL10 in supernatants from WT splenic B cells stimulated with (black) or without (white) R848 as in (**A**). (**C**) ELISA measured CXCL10 in day 4 serum of WT mice with (black) or without (white) i.p. injection of 50μg R848 on day 0 and day 3. (**D**-**E**) GTT and glucose area under curve (AUC) for WT mice fed the NCD (**D**, circles) or HFD (**E**, squares), with (black) or without (white) transfer of B cells enriched for T-bet^{+} CD11c^{+} B cells. Donor B cells were from WT mice treated with R848 and NP-KLH *in vivo* prior to isolation/transfer. See also Figure S5. Bar graphs show GTT AUC, 4 days after transfer. Data are from one experiment with at least 4 mice/grp (**A**), pooled from three experiments (**B**-**C**), or from 2 experiments with 2–4 mice/grp (**D**-**E**). Symbol centers or bar heights indicate individual values or group means, respectively and data show mean ± SEM; (**A**-**E**) Student's t-test; *p < 0.05, **p < 0.01, ***p < 0.001, ****p < 0.0001.

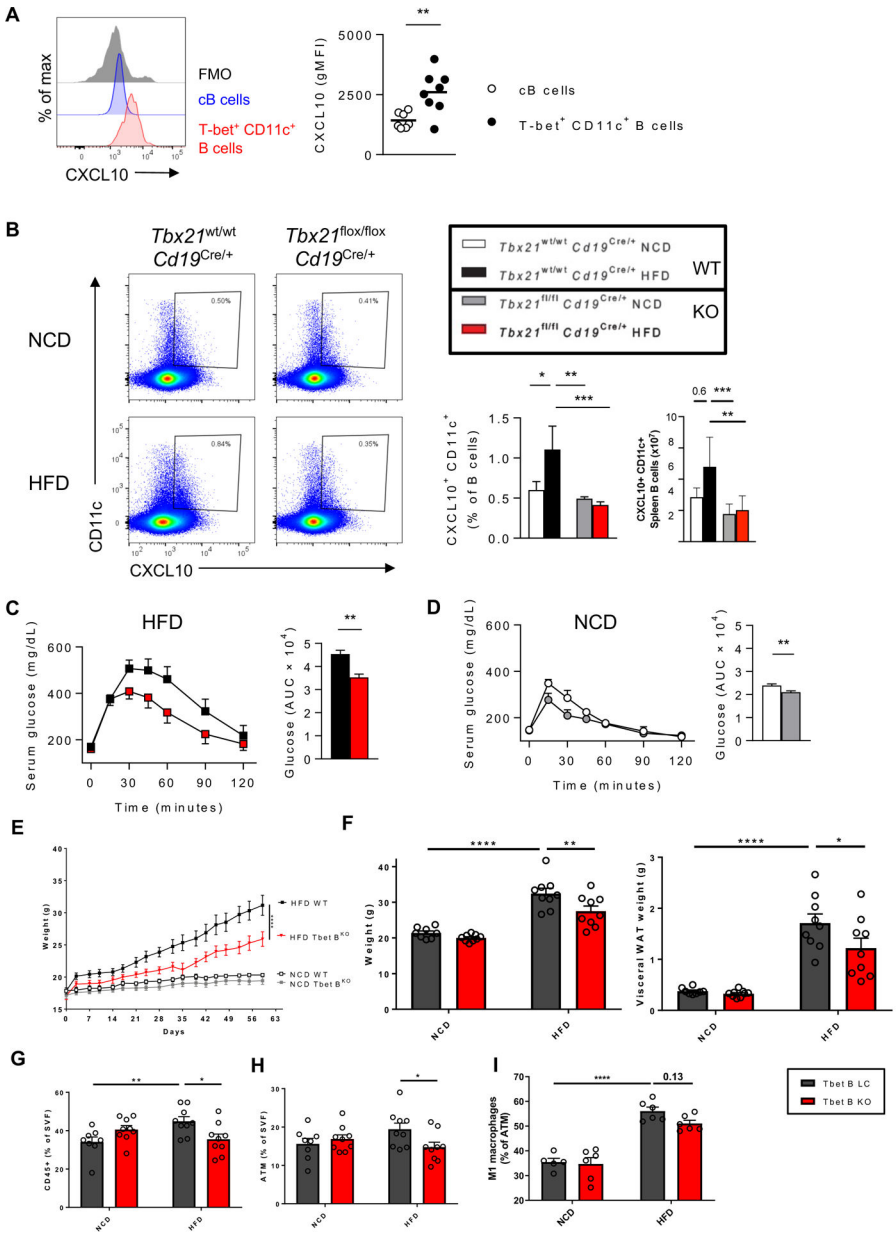

Figure 6. Ablation of *Tbx21* in B cells improves metabolic symptoms, limits adipose weight gain, and reduces inflammatory macrophage infiltrate in adipose tissue during obesity.

(**A**) Representative flow cytometry histograms and scatter plot summary of intracellular CXCL10 protein expression by Tbet+ CD11c+ B or conventional B cells (cB) as compared to fluorescent minus one (FMO) control staining. (**B**) Flow cytometry plots display gating strategy and frequency of splenic $CXCL10^{+}$ $CD11c^{+}$ B cells isolated from indicated mice fed NCD (top panels) or HFD (bottom panels); frequency summarized in bar graph. (**C-D**) GTT and glucose area under curve (AUC) for indicated mice fed HFD (**C**, squares; **E**, black squares or red triangles) or NCD (**D**, circles; **E**, white or grey squares). Bar graphs show AUC for GTT (**C,D**). Mice lacking Tbet+ B cells (red) compared to littermate controls with intact Tbet+ B cells (black) when fed a HFD vs NCD were compared for total and visceral

white adipose tissue weight (**F**) and frequency of CD45+ leukocytes (**G**), adipose tissue macrophages (ATM) (**H**), and M1 macrophages (**I**). Dots represent individual mice. Data pooled from two experiments with 3–4 mice/grp; lines and bar heights represent mean ± SEM; Student's t-test; *p < 0.05, **p < 0.01, ***p < 0.001, ****p < 0.0001.

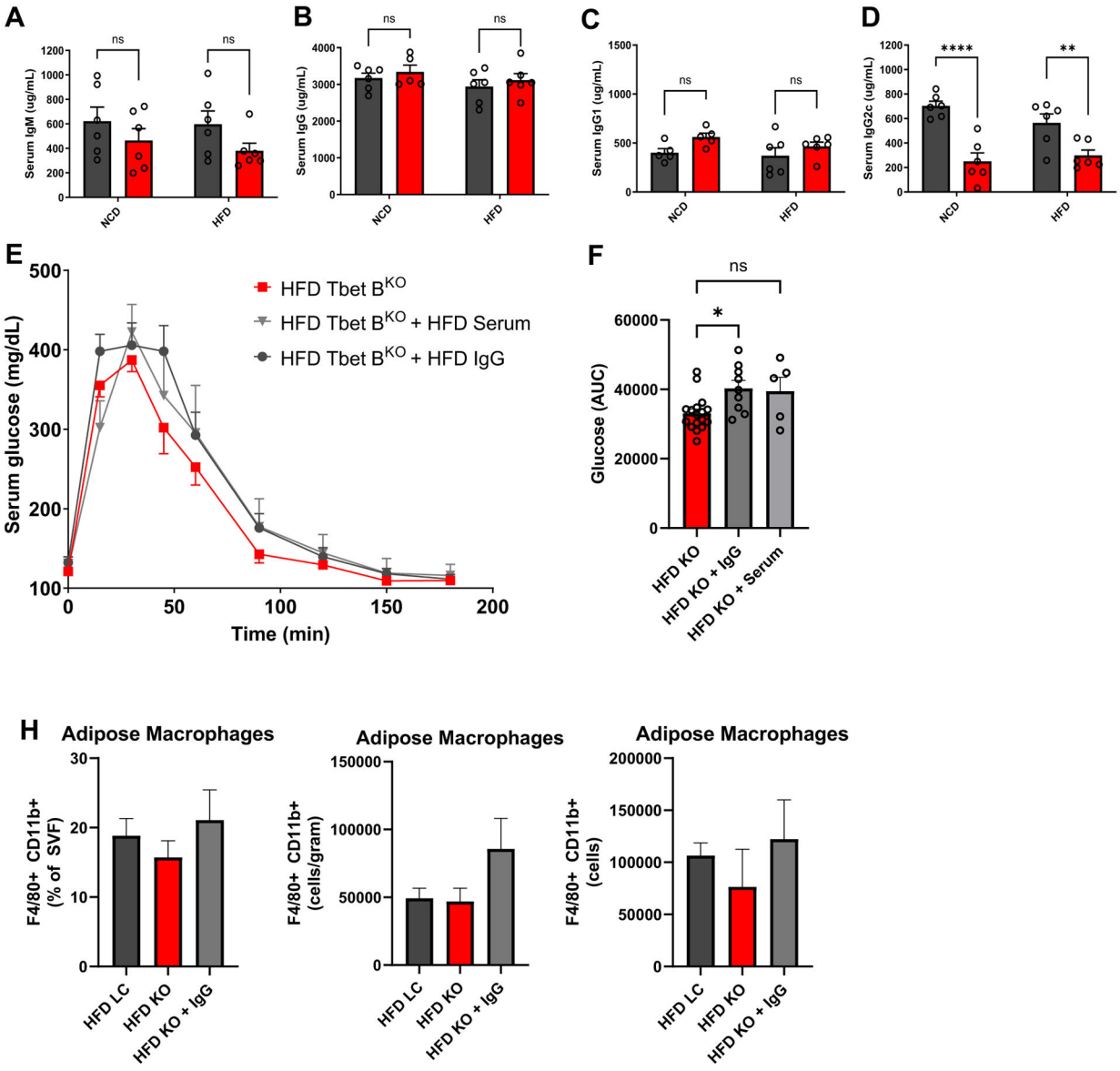

Figure 7. Mice lacking Tbet+ B cells have reduced serum IgG2c and reduced glucose intolerance, but adoptive transfer of HFD serum or purified IgG from HFD serum restores metabolic disease and expands WAT macrophages.

(A-D) ELISA on serum from Tbet+ B cell deficient mice (red) or intact littermate controls (black) fed NCD or HFD for 20+ weeks revealed concentrations (ug/ml) of total IgM (**A**), IgG (**B**), IgG1 (**C**), and IgG2c (**D**). GTT and glucose (AUC) of HFD fed Tbet+ B cell deficient mice (red square) are exacerbated by serum transfer from WT HFD fed mice (grey triangle) or purified IgG from WT HFD mice (black circle) (**E, F**). Transfer of IgG from HFD fed WT mice to obese mice lacking Tbet+ B cells restores frequency, cells/gram, and number of $F4/80^{+}CD11b^{+}$ adipose macrophages to levels comparable to HFD fed littermate controls (**H**).

KEY RESOURCES TABLE

REAGENT or RESOURCE	SOURCE	IDENTIFIER	RRID
Antibodies			
Mouse FACS			
TCRβ Brilliant Violet 510™	Biolegend	109233	AB_2562349
TCRβ Brilliant Violet 421™	Biolegend	109229	AB_10933263
TCRβ Pacific Blue	Biolegend	109226	AB_1027649
TCRβ PerCp-Cy5.5	Biolegend	109227	AB_1575176
CD45.1 Brilliant Violet 711™	Biolegend	110739	AB_2562605
CD45.1 APC	Biolegend	110713	AB_313502
CD45.2 Brilliant Violet 785™	Biolegend	109839	AB_2562604
CD45.2 PerCP-Cy™5.5	Biolegend	109827	AB_893352
CD45 BV785	Biolegend	103149	AB_2564590
T-bet PE-Cy™7	Biolegend	644823	AB_2561760
T-bet Brilliant Violet 785™	Biolegend	644835	AB_2721566
CD69 PE	Biolegend	104507	AB_313110
CD69 PE-Cy™7	Biolegend	104511	AB_493565
CD69 Brilliant Violet 421™	Biolegend	104527	AB_10900250
PLZF	Santa Cruz	SC-28319	AB_2218941
IgG1 PE-Cy™7	Biolegend	406613	AB_2562001
CD21/35 Brilliant Violet 650™	BD Biosciences	740495	AB_2740218
CD23 Brilliant Violet 510™	Biolegend	101623	AB_2563705
IgM Brilliant Violet 605™	Biolegend	406523	AB_2563358
IgD FITC	BD Biosciences	553439	AB_394859
FcRII/III (CD16/CD32) APC/Cy7	Biolegend	101328	AB_2104158
CD19 PE-Cy7	Tonbo	60-0193-U100	AB_2621840
CD19 BV421	Biolegend	115538	AB_11203527
CD19 FITC	BD Biosciences	553785	AB_395049
CD19 BV786	BD Biosciences	563333	AB_2738141
Anti-mouse CD16/32 (2.4G2)	Bio-X-Cell	CUS-HB-197	AB_2687830
PE-Cy7 Rat Anti-Mouse CD19, Clone 6D5	Biolegend	115520	AB_313655
CD11c APC	BD Biosciences Tonbo	550261 20-0114-U100	AB_398460
CD11c PE	BD Biosciences	553802	AB_395061
CD11c BV650	BD Biosciences	564079	AB_2725779
CD36 AF647	Biolegend	102610	AB_528794
CXCR3 Brilliant Violet 650™	Biolegend	126531	AB_2563160
IL-10 APC	BD Biosciences	554468	AB_398558

REAGENT or RESOURCE	SOURCE	IDENTIFIER	RRID
Nur77 PE	eBioscience	12-5965-82	AB_1257209
NK1.1 BV650	Biolegend	108736	AB_2563159
NK1.1 PE	Tonbo	50-5941	AB_2621804
CD11b BV510	Biolegend	101263	AB_2629529
CD11b FITC	BD Biosciences	553310	AB_394774
F4/80 BV421	Biolegend	123137	AB_2563102
F4/80 BUV661	BD Biosciences	750643	AB_2874771
CD1d tetramer APC	NIH Tetramer Core		
Ghost Dye UV450	Thermofisher	L34962	
B220 BV786	BD Biosciences	563894	AB_2738472
LipidTox Deep Red	Fisher Scientific	H34477	
Human FACS			
CD3 BV510	Biolegend	317332	AB_2561943
Vα24-Jα18 Brilliant Violet 421™	Biolegend	342915	AB_2564004
CD15 FITC	Biolegend	301904	AB_314196
T-bet BV785	Biolegend	644835	AB_2721566
Tbet PECy7	Biolegend	644824	AB_2561761
Isotype MOPC-21 IgG1k BV785	Biolegend	400169	AB_11219601
CD11c BV650	Biolegend	301637	AB_2562231
CD69 BV650	Biolegend	310933	AB_2561783
CD27 APC Clone O323	Tonbo	20-0279-T025	AB_2621569
CD27 Clone LG.3A10	Biolegend	124211	AB_1236460
IgD BV421	Biolegend	348225	AB_2561618
Mouse ELISA			
Total capture	Invitrogen	PA1-85986	
IgG Horseradish Peroxidase	Southern Biotech	1030-05	
IgM Horseradish Peroxidase	Southern Biotech	1020-05	
IgG1 Horseradish Peroxidase	Southern Biotech	1070-05	
IgG2b Horseradish Peroxidase	Southern Biotech	1090-05	
IgG2c Horseradish Peroxidase	Southern Biotech	1078-05	
IgG3 Horseradish Peroxidase	Southern Biotech	1100-05	
IgA Horseradish Peroxidase	Southern Biotech	1040-05	
IgE Horseradish Peroxidase	Southern Biotech	1110-05	
Human ELISA			
Total capture	Southern Biotech	2010-01	
IgG Horseradish Peroxidase	Jackson ImmunoResearch Inc.		
IgM Horseradish Peroxidase	Southern Biotech	2020-05	

REAGENT or RESOURCE	SOURCE	IDENTIFIER	RRID
IgG1 Horseradish Peroxidase	Southern Biotech	9052-05	
IgG2 Horseradish Peroxidase	Southern Biotech	9060-05	
IgG3 Horseradish Peroxidase	Southern Biotech	9210-05	
IgG4 Horseradish Peroxidase	Southern Biotech	9200-05	
IgA Horseradish Peroxidase	Jackson ImmunoResearch Inc.		
IgE Horseradish Peroxidase	Southern Biotech	9160-05	
Rabbit Serum	Fisher Sigma	ICN1935780 R4505-500	
Goat Serum	Sigma	G6767	
Bacterial and Virus Strains			
Biological Samples			
Human samples	San Antonio Plastic Surgery Institute/Christus Santa Rosa Hospital		
Chemicals, Peptides, and Recombinant Proteins			
Alpha Galactosyl-Ceramide KRN7000	Enzo Life Sciences Avanti Polar lipids	Cat# BML-SL232 867000P-1mg	
Resiquimod	Sigma	SML0196-10MG	
CD1d-tetramers	NIH Tetramer Core Facility	N/A	
Brefeldin A (GolgiPlug)	Biolegend	420601	
FBS	Cytiva	SH30088.03	
L-Glutamine	Fisher	25-005-CI	
RPMI 1640 medium	Fisher	MT10040CV	
Collagenase	Sigma	C5138-5G	
Streptavidin-Horseradish Peroxidase	Fisher BD Pharmingen	SNN2004 (nowS911) 554066	
Glucose	Sigma	G8769-100ML	
Formalin	Fisher	22-050-104	
OCT	Fisher	23-730-571	
NP-KLH	Biosearch Technologies	N-5060-5	
DMEM	Fisher	MT10014CV	
BSA	Lee Biosolutions	100-12	
PBS	Fisher	BP243820	
Critical Commercial Assays			
CXCL10 ELISA	R&D systems	DY466-05	
Foxp3 / Transcription Factor Staining Buffer Set	eBioscience	Cat# 00-5523-00	
LIVE/DEAD Fixable Near-IR Dead Cell Staining Kit	Life Technologies	Cat# L10119	
B cell isolation kit	StemCell	19854	

REAGENT or RESOURCE	SOURCE	IDENTIFIER	RRID
Melon Gel IgG Spin	ThermoFisher	45206	
Pierce Protein Concentrators PES, 50K MWCO	ThermoFisher	88538	
Deposited Data			
Experimental Models: Cell Lines			
Experimental Models: Organisms/Strains			
Mouse: Wild type C57BL/6J	The Jackson Laboratory	Strain Code: JAX 000664	
Mouse: WT Congenic (CD45.1) B6.SJL-Ptprca Pepcb/BoyJ	The Jackson Laboratory	Strain Code: JAX 002014	
Mouse: GREAT C.129S4(B6)-Ifng$^{tm3.1Lky}$/J	Markus Mohrs	Strain code: JAX 017580	
Mouse: Vα14tg C57BL/6-Tg(Cd4-TcraDN32D3)1Aben/J	Michael Brenner; The Jackson Laboratory	Strain Code: JAX 014639	
Mouse: B6.SJL B1–8^{hi} B6.129P2 (C)-Ighg^{tm12Cgn}/J	Michel Nussenzweig	Strain code: JAX 12642	
Mouse: C57BL/6 Jα18−/−	Michael Brenner	N/A	
Mouse: CD1d−/− B6.129S6-Del(3Cd1d2-Cd1d1)1Sbp/J	Mark Exley; The Jackson Laboratory	Strain Code: JAX 008881	
Mouse: Tbet$^{fl/fl}$ B6.129-*Tbx21*^{tm2Srnr}/J mice	Nu Zhang; The Jackson Laboratory	Strain Code: JAX 022741	
Mouse: CD19^{Cre} C.Cg-Cd19tm1(cre)Cgn Ighb/J	The Jackson Laboratory	Strain Code: JAX 004126	
Mouse: T-bet$^{fl/fl}$ CD19$^{cre/+}$; C.Cg-Cd19tm1(cre)Cgn Ighb/J crossed with B6.129-*Tbx21*^{tm2Srnr}/J mice	This paper	N/A	
Mouse: CXCL10−/− C.129S4(B6)-Cxcl10^{tm1Adl}/J	The Jackson Laboratory	Strain code: JAX 006087	
Oligonucleotides			
Primer Tbx21 Forward: 5'-AACTGTGTTCCCGAGGTGTC-3'			
Primer Tbx21 Reverse: 3'-GGAGCCCACAAGCCATTACA-3'			
Recombinant DNA			
Software and Algorithms			
GraphPad Prism v7	GraphPad	https://www.graphpad.com/scientific-software/prism/	
FlowJo (version 10.1)	FlowJo, LLC	https://www.flowjo.com	
MS Excel 2016	Microsoft	N/A	

REAGENT or RESOURCE	SOURCE	IDENTIFIER	RRID
Diva	BD Biosciences	http://www.bdbiosciences.com/us/instruments/clinical/software/flowcytometry-acquisition/bd-facsdivasoftware/m/333333/overview	
Other			
High Fat Diet (HFD; 60% kcal fat)	Research Diets	D12492	
FACS analyzer	BD Bioscience	BD FACSCelesta	
FACS sorter	BD Bioscience	BD FACSAriaIIIb	
100 μm cell strainer	Fisher	22-363-549 08-771-19	
40 μm cell strainer	Fisher	22-363-547 08-771-1	
Crysostat microtome	Leica	VT1000S	
Glucose strips	Bayer Contour	7097C	
Glucometer	Bayer Contour	9545C	